

**COMPUTATIONAL DESIGN STRATEGY OF  
PHARMACEUTICAL CO-CRYSTALS: A CASE STUDY OF  
ANTI-CANCER DRUGS**

**NADIA HANIM BINTI SABRI**

**FACULTY OF SCIENCE  
UNIVERSITY OF MALAYA  
KUALA LUMPUR**

**2018**

**COMPUTATIONAL DESIGN STRATEGY OF  
PHARMACEUTICAL CO-CRYSTALS: A CASE STUDY  
OF ANTI-CANCER DRUGS**

**NADIA HANIM BINTI SABRI**

**DISSERTATION SUBMITTED IN FULFILMENT OF  
THE REQUIREMENTS FOR THE DEGREE OF MASTER  
OF SCIENCE**

**DEPARTMENT OF CHEMISTRY  
FACULTY OF SCIENCE  
UNIVERSITY OF MALAYA  
KUALA LUMPUR**

**2018**

**UNIVERSITY OF MALAYA**  
**ORIGINAL LITERARY WORK DECLARATION**

Name of Candidate: Nadia Hanim Binti Sabri

Matric No: SGR140018

Name of Degree: Master of Science

Title of Project Paper/Research Report/Dissertation/Thesis ("this Work"):

Computational Design Strategy of Pharmaceutical Co-Crystal: A Case Study of Anti Cancer Drugs

Field of Study: Theoretical and Computational Chemistry

I do solemnly and sincerely declare that:

- (1) I am the sole author/writer of this Work;
- (2) This Work is original;
- (3) Any use of any work in which copyright exists was done by way of fair dealing and for permitted purposes and any excerpt or extract from, or reference to or reproduction of any copyright work has been disclosed expressly and sufficiently and the title of the Work and its authorship have been acknowledged in this Work;
- (4) I do not have any actual knowledge nor do I ought reasonably to know that the making of this work constitutes an infringement of any copyright work;
- (5) I hereby assign all and every rights in the copyright to this Work to the University of Malaya ("UM"), who henceforth shall be owner of the copyright in this Work and that any reproduction or use in any form or by any means whatsoever is prohibited without the written consent of UM having been first had and obtained;
- (6) I am fully aware that if in the course of making this Work I have infringed any copyright whether intentionally or otherwise, I may be subject to legal action or any other action as may be determined by UM.

Candidate's Signature

Date:

Subscribed and solemnly declared before,

Witness's Signature

Date:

Name:

Designation:

# [COMPUTATIONAL DESIGN STRATEGY OF PHARMACEUTICAL CO-CRYSTALS: A CASE STUDY OF ANTI-CANCER DRUGS]

## ABSTRACT

Thymidylate synthase (TS) is a biomarker for fluoropyrimidine-based chemotherapy that provides the sole intracellular *de novo* source of thymidylate, an essential precursor to DNA synthesis. Antifolate drug and fluoropyrimidine-based drug have potential to disrupt TS activity by nucleotide and antifolate binding sites. Raltitrexed (tomudex) is one of the antifolate drugs that inhibit TS by decreasing dihydropyrimidine dehydrogenase (DHFR) activity. Fluoropyrimidine-based drug remains the most effective first-line treatment for colorectal cancer (CRC) by inducing thymidylate deficiency and imbalances in the nucleotide that led to DNA incorporation. However, most of the marketed drugs including these antifolate and fluoropyrimidine-based drugs have the lack of efficiency due to low solubility and dissolution rate. This research highlights an area in the computational chemistry of dual-drug co-crystals to improve drug delivery by modifying their physical properties. The combination treatment of raltitrexed with other anti-cancer agents has been verified through several types of research. Thus, the potential of co-crystals as the cancer inhibitors in the presence of raltitrexed have been carried out in this study. This present work discovered the combination of raltitrexed with modified 5-FU based co-crystal (compound 1) that gave a significant benefit of effectiveness and manageable toxicity via computational approach. The molecular dynamics simulation results suggested that the compound 1 enhancing binding strength of raltitrexed to inhibit TS with binding free energy (-45.68 kcal/mol) compared to raltitrexed alone (-16.57 kcal/mol).

Keywords: raltitrexed, 5-Flourouracil (5-FU), compound 1, thymidylate synthase (TS), molecular dynamics simulation.

**[STRATEGI REKA BENTUK PENGKOMPUTERAN UNTUK  
FARMASEUTIKAL KO-KRISTAL: KAJIAN KES UBATAN ANTI-KANSER]**

**ABSTRAK**

*Thymidylate synthase* (TS) merupakan “biomarker” untuk kemoterapi berasaskan floropirimidin yang membekalkan sumber tunggal intrasel *de novo* kepada thymidylate, pelopor penting bagi sintesis DNA. Ubat antifolat dan ubat berasaskan floropirimidin mempunyai potensi untuk mengganggu aktiviti TS melalui kawasan ikatan nukleotida dan antifolat. Raltitrexed (tomudex) adalah salah satu ubat antifolat yang menghalang TS dengan menurunkan aktiviti dehidrogenas dihydropyrimid (DHFR). Ubat berasaskan floropirimidin kekal sebagai perubatan utama yang paling berkesan untuk kolorektal kanser dengan mendorong kekurangan thymidylate dan ketidakseimbangan dalam nukleotida yang membawa kepada penggabungan DNA. Walaubagaimanapun, kebanyakan ubat-ubatan di pasaran termasuk ubat antifolat dan ubat berasaskan floropirimidin ini kurang berkesan kerana kadar kelarutan dan pembubaran yang rendah. Kajian ini akan menekankan dwi-ubat ko-kristal dalam bidang kimia pengkomputeran bagi meningkatkan penyampaian ubat dengan mengubah sifat-sifat fizikal mereka. Kombinasi rawatan raltitrexed bersama ejen anti-kanser telah disahkan melalui beberapa jenis kajian. Oleh itu, potensi kristal bersama sebagai perencat kanser dengan kehadiran raltitrexed telah dijalankan dalam kajian ini. Kajian ini menemui kombinasi raltitrexed dengan 5-flourourasil (5-FU) berasaskan ko-kristal yang telah diubah suai (sebatian 1) memberi manfaat yang signifikan kepada keberkesanan dan ketoksikan yang boleh diurus melalui kaedah pengkomputeran. Hasil simulasi dinamik molekul menunjukkan bahawa sebatian 1 dapat meningkatkan kekuatan mengikat raltitrexed untuk menghalang TS dengan tenaga pengikatan bebas (-45.68 kcal / mol) berbanding raltitrexed sahaja (-16.57 kcal / mol).

Kata kunci: raltitrexed, 5-Flourourasil (5-FU), sebatian 1, thymidylate synthase (TS), simulasi dinamik molekul.

University of Malaya

## ACKNOWLEDGEMENTS

Gratitude to Allah Almighty who provided me the strength to conduct the research on this issue and complete this thesis. It has been a period of intense learning for me, not only in the scientific arena but also on my personal level.

First and foremost, my sincere appreciation to my supervisor, Assoc. Prof. Dr. Vannajan Sanghiran Lee and my co-supervisor; Prof. Dr. Shariffudin Bin Md Zain and Dr. Siti Nadiah Binti Halim for their patience, motivation, enthusiasm and immense knowledge. Their guidance helped me to complete my research and writing of this thesis.

My sincere gratitude also to my fellow lab mates in the Computational Chemistry Laboratory Group for their help, advice and moral support. In addition, I want to thank my family especially my parents for supporting me spiritually throughout my life.

Last but not least, to everyone who have been with me in every aspect in recent years in completing this thesis.

## TABLE OF CONTENTS

Abstract.....	iii
Abstrak.....	iv
Acknowledgements.....	vi
Table of Contents.....	vii
List of Figures.....	xi
List of Tables.....	xiii
List of Symbols and Abbreviations.....	xiv
 <b>CHAPTER 1: INTRODUCTION.....</b>	 <b>1</b>
1.1 Issues in Pharmaceutical Industry.....	1
1.2 Co-crystals.....	1
1.3 Pharmaceutical Co-crystal.....	2
1.4 Colorectal Cancer.....	3
1.5 Thymidylate Synthase.....	4
1.6 Drug Design.....	4
1.7 Problems Statement.....	5
1.8 Objectives of Research.....	5
 <b>CHAPTER 2: LITERATURE REVIEW.....</b>	 <b>7</b>
2.1 Crystal.....	7
2.1.1 Co-crystal versus Salt.....	7
2.1.2 Molecular Co-crystals (MCCs).....	8
2.1.3 Crystal Engineering and Supramolecular Chemistry.....	8
2.1.4 Supramolecular Synthon.....	9
2.1.5 Pharmaceutical Co-crystal.....	10

2.1.5.1	Target Active Pharmaceutical Ingredient (API).....	11
2.1.5.2	Conformer Selection.....	12
2.2	Colorectal Cancer (CRC).....	13
2.2.1	Risk Factors to Acquire CRC.....	13
2.2.1.1	Lifestyle-related factors.....	13
2.2.1.2	Hereditary.....	13
2.3	Thymidylate Synthase (TS).....	14
2.3.1	Structure, Dynamics and Conformational Changes of TS.....	14
2.3.2	Thymidylate Synthase Mechanism Pathway.....	17
2.3.3	Chemical Mechanism in TS Reaction.....	18
2.3.4	Inhibition of Thymidylate Synthase.....	19
2.3.4.1	Fluoropyrimidine-based Drug and Prodrug.....	21
2.3.4.2	Antifolate Drug.....	22
2.3.4.3	Combination Therapies.....	23
2.4	Computational Approach in Drug Design.....	23
2.4.1	Protein-Ligand System.....	24
2.4.2	Molecular Docking.....	24
2.4.3	Molecular Dynamics Simulation.....	27
2.4.3.1	General Amber Force Field (GAFF).....	27
2.4.3.2	Molecular Mechanics/ Poisson-Boltzmann Surface Area (MM-PBSA) and Molecular Mechanics/Generalized Born Surface Area (MM-GBSA).....	28
2.4.4	2D Quantitative Structure- Activity Relationship (2D QSAR).....	29
2.4.4.1	Lipinski's Rule of Five.....	29
2.4.4.2	Absorption, Distribution, Metabolism, Elimination and Toxicity (ADMET) Prediction.....	30
2.4.5	Factors Affecting Protein-Ligand Binding Affinity.....	30
2.4.5.1	Non-Covalent Interactions.....	31

2.4.5.2	Desolvation.....	33
2.4.5.3	Flexibility of Receptor.....	33
<b>CHAPTER 3: METHODOLOGY.....</b>		<b>34</b>
3.1	The Classification of Ligands.....	34
3.2	The Potential of Co-crystal as Anti-cancer Inhibitor.....	36
3.2.1	Molecular Docking Studies of Protein-Ligand Systems.....	36
3.2.2	Molecular Dynamics of Protein-Ligand Complexes.....	37
3.2.3	Binding Free Energy Calculation and Per-residue Free Energy Decomposition.....	39
3.3	Modification to Enhance Potential of Co-crystal to Inhibit TS.....	39
3.3.1	Fragment Linking Approach.....	39
3.3.2	Molecular Docking Study.....	40
3.3.3	Molecular Dynamic Simulation.....	41
3.3.4	Binding Free Energy Calculation and Per-residue Free Energy Decomposition.....	42
3.4	Insight into Protein-Ligand Interaction.....	42
3.5	Drug-likeness Analysis.....	43
3.5.1	Physicochemical Properties Prediction.....	43
3.5.2	2D QSAR by ADMET Prediction.....	43
<b>CHAPTER 4: RESULT AND DISCUSSION.....</b>		<b>45</b>
4.1	The Potential of Co-crystals and Compound 1 as the Cancer Inhibitors.....	45
4.1.1	Molecular Docking Study.....	45
4.1.2	Stability and Flexibility of Protein-ligand Complexes.....	51
4.1.3	Binding Free Energy Calculation (MM-PBSA/GBSA).....	54
4.1.4	Key Interactions Residues Involving in the Binding Sites of the Complexes .....	56

4.2	Drug-likeness Analysis.....	62
4.2.1	Physicochemical Properties Prediction based on Lipinski's Rule of Five (RO5).....	62
4.2.2	ADMET Prediction for 2D QSAR.....	62

## **CHAPTER 5: CONCLUSION..... 66**

## **REFERENCES..... 67**

## **List of Publications and Papers Presented..... 79**

University of Malaya

## LIST OF FIGURES

Figure 2.1 : Possible crystal packing of API: (A) salt, (B) molecular co-crystal and (C) ionic co-crystal (modified from Byrn et al., 1999).....	8
Figure 2.2 : (A)Supramolecular homosynthons, carboxylic acid homosynthon (B)Supramolecular heterosynthons, carboxylic acid-amide heterosynthon.....	10
Figure 2.3 : The structure of uracil.....	11
Figure 2.4 : The structure of 5-fluorouracil.....	11
Figure 2.5 : Structure of (A) urea and (B) thiourea.....	12
Figure 2.6 : The structure of (A)2,2-bipyridine and (B)4,4-bypiridine.....	12
Figure 2.7 : X-ray structure of hTS/dUMP(magenta)/raltitrexed (cyan) complex (pdb id: 1HVY) and active site loop (yellow) (Phan et al., 2001). ....	16
Figure 2.8 : The interaction for the catalytic cysteine, Cys195 (blue stick) with dUMP (magenta stick) and raltitrexed (cyan stick) in active site loop (yellow ribbon) of hTS complex.....	17
Figure 2.9 : Biosynthesis pathways of TS (modified from Wilson et al., 2014). ....	18
Figure 2.10 : Chemical mechanisms of TS (Carreras et al., 1995).....	19
Figure 2.11 : The mechanism of TS inhibition (modified from Wilson et al., 2014).....	20
Figure 2.12 : The illustration of molecular docking for protein-ligand system (modified from Alejandra et al., 2013). ....	25
Figure 2.13 : The predominant types of non-bonded interaction in the protein- complex (modified from Bleicher et al, 2003).....	31
Figure 3.1 : The structures of (A) 5FU-U co-crystal and (B) compound 1.....	40
Figure 3.2 : The 2D structure of compound 1.....	40
Figure 4.1 : The overall docking structures and superimpositions of the ligands for all complexes where dUMP (light blue), 5FU-U co-crystal (red), 5FU-TU co-crystal (green), 5FU-22 (orange),5FU-44 (blue), UU (purple), compound 1 (yellow) and raltitrexed (pink).....	45
Figure 4.2 : The CDOCKER interaction energy of complexes in kcal/mol.....	46

Figure 4.3 : The intermolecular hydrogen bonds (green dotted line) in the docked complexes where (A)raltitrexed(pink)-dUMP(light blue) complex, (B)raltitrexed-5FU-U co-crystal(red) complex, (C) raltitrexed-5FU-TU co-crystal(green) complex, (D) raltitrexed-5FU-22 co-crystal (orange) complex, (E) raltitrexed-5FU-44 co-crystal(blue) complex, (F) raltitrexed-UU co-crystal(purple) complex and (G) raltitrexed-compound 1 (yellow) complex.....	48
Figure 4.4 : Molecular dynamic trajectory plot correlating root mean square deviation (Å) of raltitrexed-5FU-U co-crystal complex, raltitrexed-compound 1 complex and raltitrexed-dUMP complex within 75 ns simulation.....	53
Figure 4.5 : Inspection of individual frame in raltitrexed-5FU-U co-crystal complex along the simulation.....	54
Figure 4.6 : Key interaction residues within 4 (Å) in the nucleotide binding site that contribute to the binding strength of complexes.....	57
Figure 4.7 : Key interaction residues within 4 (Å) in the folate binding site that contribute to the binding strength of complexes.....	58
Figure 4.8 : The percentage of hydrogen bonds occupied per residue within last 5 ns.	59
Figure 4.9 : The non-covalent interaction for (A)raltitrexed(pink)-dUMP(light blue) complex and (B)raltitrexed-compound 1(yellow) complex at 75 ns trajectory. ....	61
Figure 4.10 : 2D polar surface area (PSA_2D) for each compound is plotted against their corresponding calculated atom-type partition coefficient (ALogP98) based on absorption model the 95% and 99% confidence limit ellipses corresponding to the Blood Brain Barrier(BBB) and Intestinal Absorption Model (Egan et al., 2000). ....	64

## LIST OF TABLES

Table 3.1 : The system of ligands.....	34
Table 4.1 : MM-PBSA/GBSA calculation within last 5 ns MD simulations. ....	55
Table 4.2 : Physicochemical properties prediction of ligands. ....	62
Table 4.3 : ADMET prediction of ligands.....	63

University of Malaya

## LIST OF SYMBOLS AND ABBREVIATIONS

5-FU	:	5-Fluorouracil
5'dFCR	:	5'-deoxy-5-Fluorocytidine
5'dFUR	:	5'-deoxy-5-Fluorouridine
ADMET	:	Adsorption, Distribution, Metabolism, Excretion and Toxicity
APC	:	Adenomatous Polyposis Coli
API	:	Active Pharmaceutical Ingredient
BBB	:	Blood Brain Barrier
CADD	:	Computer-Aided Drug Design
CNS	:	Central Nervous System
CRC	:	Colorectal Cancer
DHF	:	Dihydrofolate
dNTP	:	Deoxynucleotide triphosphate
dTMP	:	Deoxythymidine-5'-Monophosphate
dTTP	:	Deoxythymidine Triphosphate
dUMP	:	Deoxyuridine-5'-Monophosphate
EGFR	:	Epidermal Growth Factor Receptor
ELE	:	Electrostatic Interactions
FAP	:	Familial Adenomatous Polyposis
FDA	:	Food and Drug Administration
FdUMP	:	Fluorodeoxyuridine Monophosphate
FOLT	:	Folate Transporter
FPGS	:	Folypolyglutamate Synthase
FPP	:	Finished Pharmaceutical Product
GAFF	:	General Amber Force Field

GB	:	Generalized Born
GBTOT	:	Total Binding Free Energy Calculated by the MM/GBSA Method.
Gcom	:	Free Energy of Complex
Glig	:	Free Energy of Ligand
Grec	:	Free Energy of Protein
H-bond	:	Hydrogen Bond
HIA	:	Human Intestines Absorption
HNPCC	:	Hereditary Non-Polyposis Colorectal Cancer
HTS	:	High-Throughput Screening
hTS	:	Human Thymidylate Synthase
KA	:	Association Constant
KD	:	Dissociation Constant
LV	:	Leocovorin
MCC	:	Molecular Co-crystal
MD	:	Molecular Dynamic
MM/GBSA	:	Molecular Mechanics/ Generalized Born Surface Area
MM/PBSA	:	Molecular Mechanics/ Poisson-Boltzmann Surface Area
mTHF	:	N5,10-methylenetetrahydrofolate
PB	:	Possion-Boltzmann
PBCAL	:	Polar Contribution of Solvation
PBSUR	:	Non-polar Contribution to Solvation
PBTOT	:	Total Binding Free Energy Calculated by the MM/PBSA Method.
PLIP	:	Protein-Ligand Interaction Profiler
PME	:	Particle Mesh Ewald
PPB	:	Plasma Protein Binding

PRPD	:	Phosphoribosyl Pyrophosphate
RESP	:	Restrained Electrostatic Potential
RMSD	:	Root Mean Square Deviation
RO5	:	Rule of Five
THF	:	Tetrahydrofolate
TS	:	Thymidylate Synthase
TΔS	:	Conformational Entropy
vdW	:	van der Waals
ΔE <sub>electrostatic</sub>	:	Electrostatic Energy
ΔE <sub>internal</sub>	:	Internal Energy
ΔG	:	Binding Free Energy
ΔG <sub>bind</sub>	:	Binding Free Energy of Protein-Ligand
ΔG <sub>sol</sub>	:	Desolvation Free Energy
ΔH	:	Enthalpy
ΔS	:	Entropy
Δt	:	Time Step

## **CHAPTER 1: INTRODUCTION**

### **1.1 Issues in Pharmaceutical Industry**

The active pharmaceutical ingredient (API) can be defined as a substance that have pharmacological activity or explicit impact to diagnosis, cure, mitigation, treatment or prevention of disease, or to have direct effect in modifying physiological functions in human beings (WHO, 2011). However, less than 1% active pharmaceutical ingredient reaches the market. The poor biopharmaceutical properties are the key factors for the Ssolubility issue is the major challenge in the pharmaceutical industry where the drugs are often discarded during production due to low solubility (Blagden et al., 2007).

The withdrawal and subsequent reformulation of a capsule formulation marketed under the trade name Norvir<sup>®</sup> caused by reduced solubility of polymorph (Bauer et al., 2001). Thus, enhancing the solubility and dissolution rate of the drugs is currently the focus in the pharmaceutical industry. Many studies were conducted as an effort to enhance the solubility via several approach including micronisation (Cho et al., 2010; Li et al., 2006; Rasenack et al., 2003), salt formation (Umeda et al., 2009), emulsification (Hong et al., 2006; Torchilin, 2007), solubilisation by using co-solvents (Amin et al., 2004), and the use of polymer drug vehicles to deliver poor soluble drugs (Yue et. al., 2010). The crystal engineering research on the pharmaceutical co-crystals started as an alternative to improve and overcome the stability and solubility problem of drug (Almarsson, 2004; Aakeroy, 2005).

### **1.2 Co-crystals**

Co-crystal can be classified as a structurally homogeneous co-crystalline material that consists of two or more components present in definite stoichiometric amounts (Aakeroy & Salmon, 2005). The co-crystal has been studied for more than 160 years.

The first reported co-crystal, quinhydrone was discovered by Friedrich Wohler in 1844 comprising 1:1 molar combination of components (Wohler, 1844). The concept of crystal engineering was made known by Pepinsky in 1955 and Schmidt (Pepinsky, 1955; Schmidt, 1971) implemented in the context of organic solid-state photochemical reactions. The classifying of co-crystal based on the type of conformer dates back to 1922 (Pfeiffer, 1922). It can be classified into two classes, which are molecular co-crystal (MCC) or ionic co-crystal (ICC) depending on the nature of the conformer. MCC has contained two or more different neutral conformers in a stoichiometric ratio and typically sustained by the hydrogen bonds or halogen bonds whilst ICC are typically sustained by charge-assisted hydrogen bonds and/or coordination bonds are sustaining the ICC (Coates et al., 1998; Braga et al., 2010).

### **1.3 Pharmaceutical Co-crystal**

Understudied class of crystalline solid has attracted interest from crystal engineering and pharmaceutical scientist in the drug development. Pharmaceutical co-crystal is a co-crystal whereby one of the components of the co-crystal is Active Pharmaceutical Ingredient (API) and the other components are called conformer in definite stoichiometric ratio. From the definition, it is clearly noted that solid-state API hydrates can co-crystallize with a solid conformer to form co-crystal (Cheng et al., 2009). According to Food and Drug Administration (FDA), a pharmaceutical co-crystal consists of an API with a neutral guest compound (also referred as conformer) in the crystal lattice whilst a co-crystal's component is in a neutral state and they have to interact via nonionic interaction (FDA, 2011).

Interestingly, the physicochemical properties can be modified without covalent modification of a drug molecule via a pharmaceutical co-crystal. The most reported pharmaceutical co-crystals fall into molecular co-crystal category. Etter, a scientist, has

extensively studied a hydrogen bond as a designed element for the preparation of multi-component co-crystal in 1990s. Her research contributed to the co-crystal field for determining the propensity for hydrogen bond interaction (Etter, 1989). In addition, a pharmaceutical co-crystal offers potential enhancement in the solubility, dissolution rate, bioavailability and physical stability (Lu et al., 2009). In year 1974, Higuchi and Ikeda used a molecular co-crystal to improve the performance of a digoxin, drug for treatment of mild to moderate heart failure, which has low bioavailability and dissolution rate. The researchers found that the solubility of digoxin increases in the presence of hydroquinone (Higuchi & Ikeda, 1974).

#### **1.4 Colorectal Cancer**

Colorectal cancer (CRC) is one of the most common malignancies that begin in the colon or rectum. Most of the colorectal cancer is an adenocarcinoma, which begins in the cells. This cancer often begins as a growth called a polyp, which may form on the inner wall of the colon or rectum. Statistics by the United State National Cancer Institute in 2015 revealed that 93,090 new cases were reported while 49,700 people died caused by the aforementioned cancer (NIH, 2015). This cancer also possess serious problem in Asian countries (Cheung et al., 2008; Ji et al., 1998; Kuriki et al., 2006; Yee et al., 2009; Yiu et al., 2009). World Health Organization (WHO) reported that the incidence of CRC is rising rapidly in the region of Asia countries such as China, Japan, South Korea and Singapore (Yiu et al., 2009; Tamura et al., 1996; Lu et al., 2003, Yang et al., 2004). In Malaysia, colorectal cancer is the second most common cancer affecting about 2900 Malaysians each year and commonly affects Malaysian men across all age groups (NCSM, 2015). The above statistics showed that CRC is a serious problem across the globe and it is rising rapidly over few decades.

## 1.5 Thymidylate Synthase

Thymidylate synthase (TS) is a target for cancer chemotherapy as the TS-catalyzed enzymatic role that provides the sole intracellular *de novo* source of thymidylate, which is an essential precursor for DNA synthesis (Appelt et al., 1991; Danenberg, 1977; Hardy et al., 1987). TS catalyzes the reductive methylation of deoxyuridine-5'-monophosphate (dUMP) to deoxythymidine-5'-monophosphate (dTMP) by using 5,10-methylenetetrahydrofolate (5,10-CH<sub>2</sub> THF) which is the only pathway for *de novo* synthesis of dTMP and DNA synthesis (Triest et al., 1999). dTMP is a subsequently phosphorylated to deoxythymidine triphosphate (dTTP) which is an essential precursor for DNA replication and repair. Its overexpression in various tumor types makes it an excellent target for chemotherapeutic intervention. The nucleotide (dUMP) and folate (5,10-CH<sub>2</sub> THF) are potential binding sites TS activity disruption (Wilson et al., 2014).

## 1.6 Drug Design

Computational techniques are widely used as a significant part of the drug design that enhances the success rate to design the potential lead compound and drugs in the drug discovery. The design of a new drug involves the following steps:

- Target identification and validation of the specific target for treatment of given disease.
- Hit discovery from high throughput screening. For example, molecular docking of a set of compounds from database to the protein.
- Hit-to-lead conversion, the preliminary optimization of the promising ligands to find the lead compounds that can be useful for further development.
- Lead optimization, the modification of the selected lead compound to enhance its adsorption, distribution, metabolism, excretion and toxicity (ADMET) properties.

- Pre-clinical test by using an animal model to establish pharmacodynamical, pharmacokinetics and ADMET properties of the drug.
- Clinical trials that performed on the patients with the aim to determine the actual therapeutic effects, toxicity of the drug, appropriate therapeutic dosage, side effects and interaction with other drugs.

A computational approach is an alternative approach that would lower the cost, shorten the time and minimize the risk associated with new substances. Molecular modelling methods can fulfilled some of the requirement of the drug design process and can be applied to overcome the biological problems. A compound may be a selective inhibitor of an enzyme but has limited therapeutically use if it does not cross the biological barriers, insoluble, unstable or accumulates in the body. Over the past few years, modelling and prediction of protein-ligand interactions have been extensively established via a computational method. Three approaches are widely used for protein-ligand interaction predictions, which are docking and scoring method, MM-PBSA/GBSA method and free energy calculations method (Mobley et al., 2009).

## **1.7 Problems Statement**

A series of the co-crystals were synthesized by Nadzri and co-workers (Nadzri et al., 2016) to overcome the poor bioavailability problems of market drugs. Hence, computational-aid drug design approach has been used to predict the potential of co-crystals to inhibit cancer specifically for colorectal cancer.

## **1.8 Objectives of Research**

This research embarks the following objectives:

- To perform molecular docking studies and molecular dynamics of the co-crystals in the present of raltitrexed as novel anti-cancer drugs.

- ii. To computationally design and modify 5-fluorouracil (5-FU) based co-crystal in order to improve the efficiency of fluoropyrimidine – based chemotherapy, especially in terms of the toxicity and solubility.
- iii. To enhance the effectiveness of a raltitrexed via combination treatment with modified co-crystal (compound 1) and observe the property via the computational method.
- iv. To develop *in silico* approach for predicting biological properties of co-crystal inhibitors for anti-cancer via the computational method.

## CHAPTER 2: LITERATURE REVIEW

### 2.1 Crystal

The poor dissolution rate, chemical stability, low aqueous solubility, low permeability, low bioavailability and moisture uptake are intrinsic barriers to the drug delivery. These factors influence the efficiency of drug and lower the market value of a drug. Hence, a drug needs to be given orally in high doses (Yadav, 2009). The multi-component crystals such as solvates, hydrates, salts and co-crystals play crucial roles in drug design of pharmaceutical industry to overcome the problems.

#### 2.1.1 Co-crystal versus Salt

The understanding of the fundamental that differentiate the salt formation and co-crystal are necessary in pre-formulation and chemical/pharmaceutical aspect. In fact, salts and co-crystals can be considered as an opposite end of the multi-component structure (Aakeroy et al., 2007). Salt is formed when there is an acid-based reaction between the API and an acidic or basic substance by transferring of a proton from an acid to base. The proton transfer depends on the pKa values of the components.

Meanwhile, co-crystallization is a result of competing for molecular associations between similar molecules (homomers) and different molecules (heteromers) (Jayasankar et al., 2006). The components in a co-crystal exist in a definite stoichiometric ratio and assemble via the non-covalent interactions like hydrogen bond, ionic bond,  $\pi$ - $\pi$  stacking interaction or van der Waals interactions (Aakeroy & Salmon, 2005). Contrary, there is no proton transfer occurred in a co-crystallization. The difference crystal packing of co-crystal and salt is illustrated in Figure 2.1 (Byrn et al., 1999). For an example, a co-crystal of succinic acid-urea is formed when an oxygen

atom in urea molecule is bonded to a hydrogen atom in a succinic acid molecule while an oxygen atom from succinic acid is bonded to a hydrogen atom of urea.

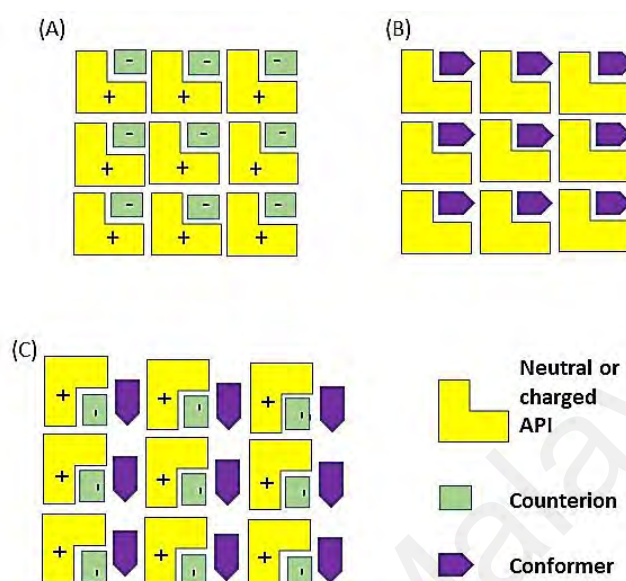


**Figure 2.1: Possible crystal packing of API: (A) salt, (B) molecular co-crystal and (C) ionic co-crystal (modified from Byrn et al., 1999).**

### 2.1.2 Molecular Co-crystals (MCCs)

The molecular co-crystal (MCC) of quinone and hydroquinone (quinhydrone) reported by Wohler (1844) was revealed to be sustained by a C=O---H-O supramolecular heterosynthon. Study on year 1974 showed peak serum digoxin concentrations for the MCC that were achieved faster than the commercialized digoxin tablets, thus reveal the potential use of MCC to enhance the performance of low solubility drug (Higuchi & Ikeda, 1974).

### 2.1.3 Crystal Engineering and Supramolecular Chemistry

Desiraju defined crystal engineering as the understanding of intermolecular interactions in the context of crystal packing, and in the utilizations of such understanding in the design of new solids with desired physical and chemical properties (Desiraju, 1995). A supermolecule is an organized, complex entity that made up of the

two or more chemical species, which are held together by intermolecular forces such as an electropositive hydrogen bond donor that moves towards an electronegative acceptor, cation-anion electrostatic interactions in complexes, and hydrophobic interactions (Vijayaraj et al., 2013).

Crystal engineering suggests the modification of the crystal packing by changing the intermolecular interaction that regulates the breaking and formation of non-covalent bonds, such as van der Waals forces,  $\pi$ -stacking, electrostatic interactions and halogen bond (Aekerooy et al., 2007). The co-crystal is designed based on few rules whereby the best proton donors and acceptors remaining after intramolecular hydrogen bond formation forms intermolecular hydrogen bonds. All proton donors and acceptors are used in hydrogen bonding and six-membered-ring intermolecular hydrogen bonds form in preference to intermolecular hydrogen bonds (Etter, 1989).

#### **2.1.4 Supramolecular Synthon**

Supramolecular synthon is defined as a structural unit within supramolecules, which can be formed by known conceivable synthetic operations involving intermolecular interaction (Desiraju, 1995). Supramolecular synthons can be classified into two types, which are supramolecular homosynthon and supramolecular heterosynthon. Supramolecular homosynthon is an interaction between the same complementary functional group such as a carboxylic acid dimer, whilst there is an interaction between the different functional group for supramolecular heterosynthon (Walsh et al., 2003). However, supramolecular heterosynthon is more relevant for the co-crystal designs since the difference in the functional group can be the driving force for the formation of co-crystal.

The systematic supramolecular heterosynthon hierarchy is a critical aspect of co-crystal engineering and co-crystal design to control the stoichiometry of co-crystal and

their existence (Duggirala et al., 2016). Carboxylic acid-amide, carboxylic acid-aromatic nitrogen, alcohol-aromatic nitrogen and alcohol-amine supramolecular heterosynthons are widely used in the research. Usually, a synthon contains an O-H...N hydrogen bond, a N-containing heterocycle and formed by a carboxylic acid (Aekerooy & Salmon, 2005).

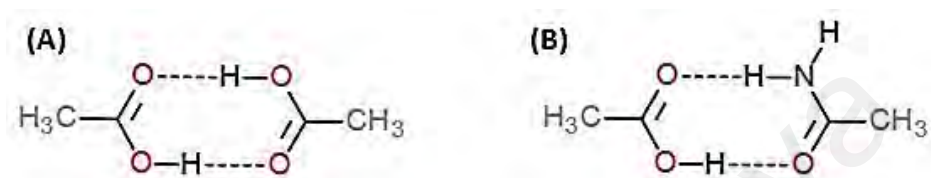


**Figure 2.2:** (A)Supramolecular homosynthons, carboxylic acid homosynthon  
(B)Supramolecular heterosynthons, carboxylic acid-amide heterosynthon.

#### 2.1.5 Pharmaceutical Co-crystal

Pharmaceutical co-crystal is a single crystalline solid formed by incorporation of two neutral molecules, an API and the co-crystal former, where co-crystal former may be an excipient or another drug (Vishwerwar et al., 2012). The study to select the suitable target of an API molecule that can form intermolecular interaction with suitable conformer has been conducted in the previous research. The ability of an API to form co-crystal is influenced by types of conformer, the API-conformer ratio, the solvents, the temperature, the pressure, and crystallization technique. In this study, the co-crystals have been synthesized via solvent drop grinding technique based on the study by Nadzri and coworkers (Nadzri et al., 2016). The solvent drop grinding technique has been reported as a cost-effective, green and reliable method for discovery of new co-crystal (Blagden et al., 2007).

#### 2.1.5.1 Target Active Pharmaceutical Ingredient (API)

a) *Uracil*



**Figure 2.3: The structure of uracil.**

Uracil is a pyrimidine derivative that plays a significant role in maintaining the structure and function of DNA and RNA. In fact, it also serves as an allosteric regulator and coenzyme for reaction in the human body. The observation from rat hepatomas radiolabeled uracil is more prominent than non-malignant tissues as indicated that there is difference in the enzymatic pathway of uracil between malignant and normal cell, thus its rationality as an anti-cancer agent is proven (Rutman et al., 1954).

b) *5-Fluorouracil (5-FU)*



**Figure 2.4: The structure of 5-fluorouracil.**

5-Fluorouracil (5-FU) is a fluoropyrimidine-based antimetabolite drug or also known as an active pharmaceutical ingredient (API) that is synthesized by Heidelberger in 1957. The hydrogen atom in position 5 of uracil is substituted by fluorine atom to occupy the active site of enzyme target and disrupt the metabolism in the malignant cells. Over the past 60 years, it is widely used for a chemotherapeutic agent with great impact to heal

various tumor types including colorectal cancer, pancreas, breast, gastric and ovarian cancers (Heidelberger et al., 1957). Furthermore, 5-FU contains both hydrogen bond donor and acceptor, which is suitable to use as a tecton, in the combination with urea, thiourea, 2,2-bipyridine and 4,4-bipyridine (Nadzri et al., 2016). Nevertheless, the incorporation actions in thymidylate synthase (TS) enzyme will increase the 5-FU cytotoxicity.

#### 2.1.5.2 Conformer Selection

##### a) *Urea and thiourea*



**Figure 2.5: Structure of (A) urea and (B) thiourea.**

Urea and its derivative, thiourea are widely used in medicine due to their great biological activities including anti-atherosclerotic, antibiotic, anti-fungal and antitumor activities (Hacbarth et al., 2002; Saeed et al., 2010). The cytotoxicity and genotoxicity are major complications of chemotherapy due to the lack of specificity of drug actions between normal and malignant cells. These complications are the concerned issues in drug development and many research have been done to solve these problems and reduce the side effect of conventional anti-tumor agents. Thus, urea and thiourea may be the alternative way as an anti-tumor agent with low toxicity (Saeed et al., 2010).

##### b) *2,2-bipyridine and 4,4-bipyridine*

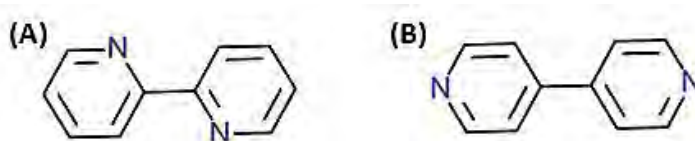


**Figure 2.6: The structure of (A)2,2-bipyridine and (B)4,4-bipyridine.**

Studies conducted posit that 2,2-bipyridine and 4,4-bipyridine are the potential anti-cancer agents. The 2,2-bipyridine derivatives are commonly used in electron-transfer process, luminescent and nanomaterials. In addition, various metal complexes consist of 2,2-bipyridine and have been reported to have anti-cancer activity (Liu et al., 2014; Gao et al., 2006).

## **2.2 Colorectal Cancer (CRC)**

Colorectal cancer (CRC) is the fourth leading cause of cancer-related death in men and the third most common in women around the world with an estimated 1.2 million new cases and 630 000 death per year of cancer patients. Asian countries such as China, Japan, South Korea and Singapore have experienced an increase of two or four folds in the incidence of CRC during the past few years. More than 95% of colorectal cancers are adenocarcinomas type, which are formed from glandular structure inside the colon and rectum (NIH, 2015).

### **2.2.1 Risk Factors to Acquire CRC**

#### **2.2.1.1 Lifestyle-related factors.**

A long-term smoker and a person that eats a large quantity red meat have high risk to acquire CRC. Heavy alcohol users tend to have CRC due to the low levels of folic acid in the body.

#### **2.2.1.2 Hereditary**

The inherited syndromes such as a gene defect (mutations) lead in developing of CRC at a younger age than usual. Familial adenomatous polyposis (FAP) and hereditary non-polyposis colorectal cancer (HNPCC) are the common inherited syndromes linked to CRC. Familial adenomatous polyposis (FAP) is a syndrome that transpires when there are mutations in the adenomatous polyposis coli (APC) gene that inherits from their parents. APC gene causes FAP by demonstrating cosegregation of mutation APC

alleles in affected kindred's (Grodin et al., 1991). In fact, FAP patients often develop extracolonic manifestations including the brain tumor. Hereditary non-polyposis colorectal cancer (HNPCC) is caused by an inherited defect of the gene MLH1 or MSH2 where both genes responsible to repair DNA damage. Patient also has a risk to develop cancer of the ovary, stomach, kidney, brain and uterus.

### **2.3 Thymidylate Synthase (TS)**

Thymidylate synthase (TS) is a significant target for a cytotoxic agent since thymidine is the only nucleotide precursor specific to DNA. It catalyzes the reductive methylation of deoxyuridine monophosphate (dUMP) by  $\text{CH}_2\text{H}_4$ -folate to produce deoxythymidine monophosphate (dTMP) and  $\text{H}_2$  folate. This reaction is an essential step to produce *de novo* 2'-deoxythymidine-5'-triphosphate (dTTP) for DNA synthesis. It is an important target for anticancer, antifungal and antiviral as disruption of TS function can inhibit the growth of proliferating cell.

Transcriptional, translational, and posttranslational mechanism influence the cellular level of TS. The differences in TS expression among human tumor cells are contributed by DNA polymorphism in the promoter region of the human TS gene (Horie et al., 1995). The previous research revealed that many types of cancer caused by overexpression of TS that can repress p53 expression by decreasing the translational efficiency of mRNA encoding this tumor suppressor protein (Ju et al., 1999). TS level is a critical determinant of response to TS inhibitor. Thus, the level of TS catalytic activity must be reduced significantly to achieve thymidylate deprivation leading to growth arrest and cell death (Johnsto et al., 1995; Davies et al., 1999; Van Triest et al., 1999).

#### **2.3.1 Structure, Dynamics and Conformational Changes of TS.**

Thymidylate synthase is a homodimeric protein with molecular weight about 63 kDa, whereby both the subunits consist of the active sites. Nevertheless, only one of the

active sites appears to be functional at a time. Briefly, TS enzyme contains two promising binding sites which are nucleotide (dUMP) and folate substrate ( $N^{5,10}$ -methylenetetrahydrofolate). In the absence of ligand, the active site of TS shows an open conformation allowing ligand to enter it.

Human TS (hTS) differs from bacterial TS for three regions: 28-29 residues and two insertions of 12- and 8- residues extend the N-terminus of hTS at the 117 and 146 positions, respectively (Carreras et al., 1995). The hTS exists in the equilibrium of active and inactive conformation. In inactive conformation, the important catalytic cysteine is twisted at almost  $180^\circ$  and points towards the dimer interface. There is a hypothesis that the inactive form of hTS interacts with its own mRNA, thus repressing TS synthesis. The active-inactive transition of hTS involves rearranging of the active-site loop consists of 181-197 residues, including catalytic cysteine (C195) as well as R185. Salo-Ahen and Wade had proven the enzymatic reaction is possible since that active site loop rotation occurs sequentially (Salo-Ahen & Wade, 2011).

The formation of the ternary complex leads to a conformational change in the protein. According to the structures of the binary complex (complex TS with dUMP) and NMR studies, it indicates that dUMP binding alone does not induce the closure of the protein and the pyrimidine ring of dUMP is located away from the catalytic Cys146 of *E.Coli* (Cys195 in human TS). This will prevent the initiation of the reaction in the absence of  $N^{5,10}$ -methylenetetrahydrofolate (mTHF). After bonding with the cofactor, the protein goes into closed conformation, thus steering of the pyrimidine ring of dUMP into the position where thiolation by Cys146 of *E.Coli* (Cys195 in human TS) can occur, and the cofactor to align for reaction with dUMP (Montfort et al., 1990).

In this study, pdb id (1HVY) as an X-ray structure of human TS-ligand-cofactor complex (ternary complex) deposited in RCSB protein data bank has been used (Figure

2.7) (Phan et al., 2001). This X-ray structure is a closed conformation of recombinant hTS complex with dUMP and Raltitrexed (Tomudex, ZD1694), as an antifolate drug at 1.9 Å resolution. There is an excellent density for the dUMP and raltitrexed (tomudex) molecule in all subunits. Nonetheless, there is a covalent bond between C6 of dUMP and catalytic Cys195. The position of the dUMP is similar to the position of nucleotide ligand that present in the ecTS/dUMP/raltitrexed and ecTS/FdUMP/CH<sub>2</sub>H<sub>4</sub> folate complexes. In addition, His196 has direct interaction with an O4 atom of the nucleotide (Phan et al., 2001). Figure 2.7 shows the active site loop (residues 181-197) is rotated approximately 180°. The interaction of the catalytic cysteine, Cys195 with dUMP is depicted in Figure 2.8.



**Figure 2.7: X-ray structure of hTS/dUMP(magenta)/raltitrexed (cyan) complex (pdb id: 1HVV) and active site loop (yellow) (Phan et al., 2001).**

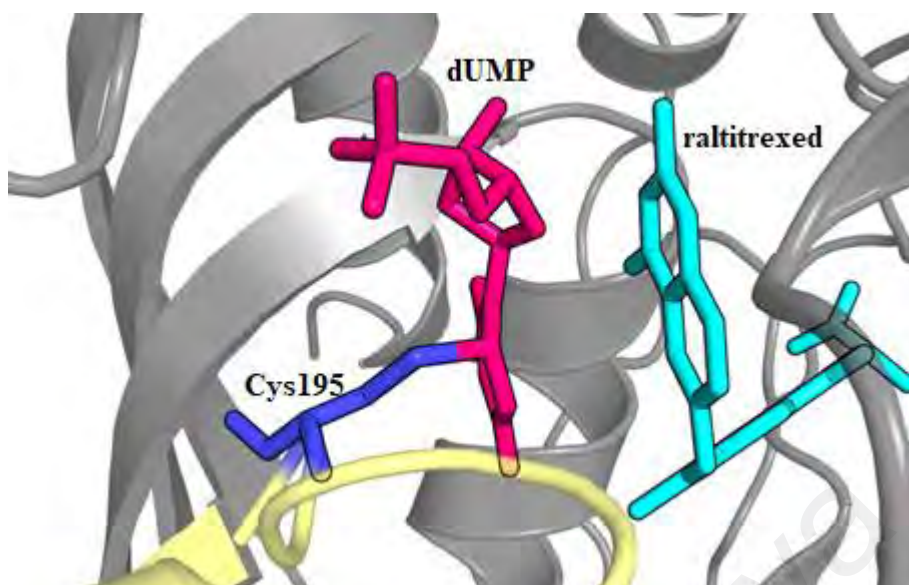


**Figure 2.8:** The interaction for the catalytic cysteine, Cys195 (blue stick) with dUMP (magenta stick) and raltitrexed (cyan stick) in active site loop (yellow ribbon) of hTS complex.

### 2.3.2 Thymidylate Synthase Mechanism Pathway

Thymidylate synthase (TS) is one of the enzymes that undergo nucleotide synthesis pathway. Consequently, TS has two stage processes to complete the synthesis cycle. First, deoxyuridine monophosphate (dUMP) binds to a receptor site that induces a configurationally change, then opens an adjacent binding site for N-5,10-methylene-tetrahydrofolate ( $\text{CH}_2\text{FH}_4$ ). A carbon group of folate is transferred to the uridine ring, yielding deoxythymidine monophosphate (dTMP) and dihydrofolate (Danenberg et al., 1978; Santi et al., 1974). dTMP is a subsequently phosphorylated by the kinase to dTDP and dTTP, one of the bases for DNA synthesis (Wilson et al., 2014).

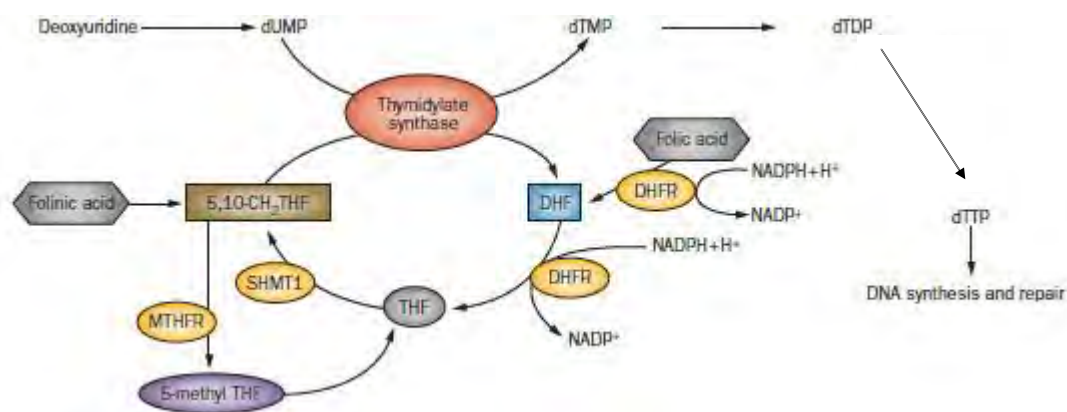


**Figure 2.9: Biosynthesis pathways of TS (modified from Wilson et al., 2014).**

### 2.3.3 Chemical Mechanism in TS Reaction

Nucleophilic catalysis was recognized in year 1968 as a feature that could simplify an apparently complex chemical reaction that was responsive to the enzyme catalysis (Santi, 1968). Basically, TS catalyses exchange 5H hydrogen atom of dUMP for a methylene group provided by mTHF, with tetrahydrofolate (THF) acting subsequently as a reductant in the reaction and undergoing transformation into dihydrofolate (DHF). Regeneration of mTHF is catalyzed by DHF reductase and serine hydroxymethyltransferase. The detail of chemical mechanisms of TS is illustrated in Figure 2.10 (Carreras et al., 1995).

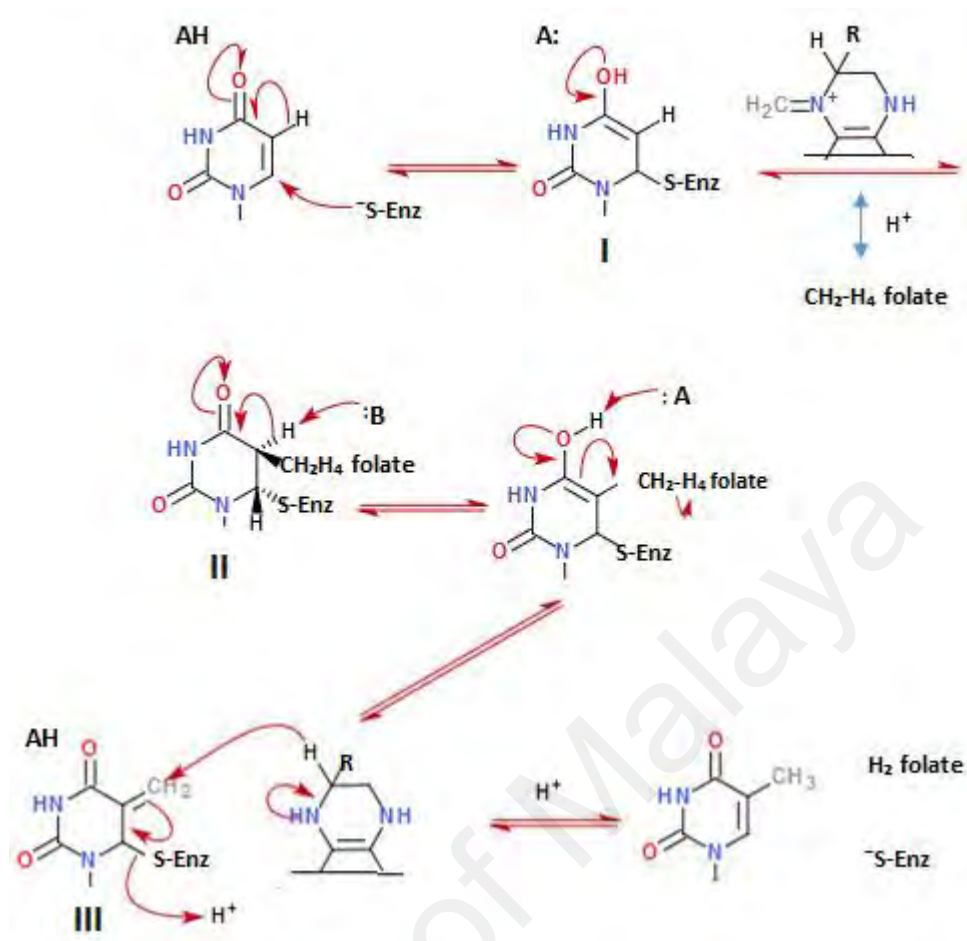


**Figure 2.10: Chemical mechanisms of TS (Carreras et al., 1995).**

After formation of the reversible ternary complex, there is the nucleophilic attack by thiol of Cys195 at the C-6 of dUMP that converts the 5-carbon to a nucleophilic enol as intermediate I. The formation of the covalently linked complex of Cys195, dUMP and the cofactor has been activated by the formation of an iminium ion at N-5. The C-5 proton of intermediate II is abstracted, followed by β-elimination of H<sub>4</sub> folate to give the exocyclic methylene intermediate III. Finally, hydride transfers from non-covalently bound H<sub>4</sub> folate to the exocyclic methylene intermediate III and β-elimination of the enzyme that produces H<sub>2</sub> folate, dTMP and the active enzyme (Carreras et al., 1995).

#### 2.3.4 Inhibition of Thymidylate Synthase

The inhibition of thymidylate synthase (TS) can be complex and vary due to the type of inhibitor, tumor type and expression levels of enzymes involved in drug metabolism.

Usually, TS inhibitors cause rapid depletion of TMP pools resulting in the subsequent depletion of TTP, which induces perturbations in deoxynucleotide triphosphate (dNTP) molecules level through feedback mechanisms. The imbalances in the cellular pool of dNTPs are thought to severely disrupt DNA synthesis and repair, resulting in cell cycle arrest and DNA damage. Furthermore, the inhibition of TS results in the accumulation of dUMP, upon sequential phosphorylation by pyrimidine monophosphate and diphosphate kinases, hence lead to the increase of deoxyuridine triphosphate (dUTP) level. Since DNA polymerases use dUTP and TTP as the substrates, excess dUTP can lead to the increased level of uracil misincorporation into DNA, resulting in severe disruption of DNA synthesis (Caradonna & Cheng, 1980). The TS inhibition mechanism is illustrated in Figure 2.11.

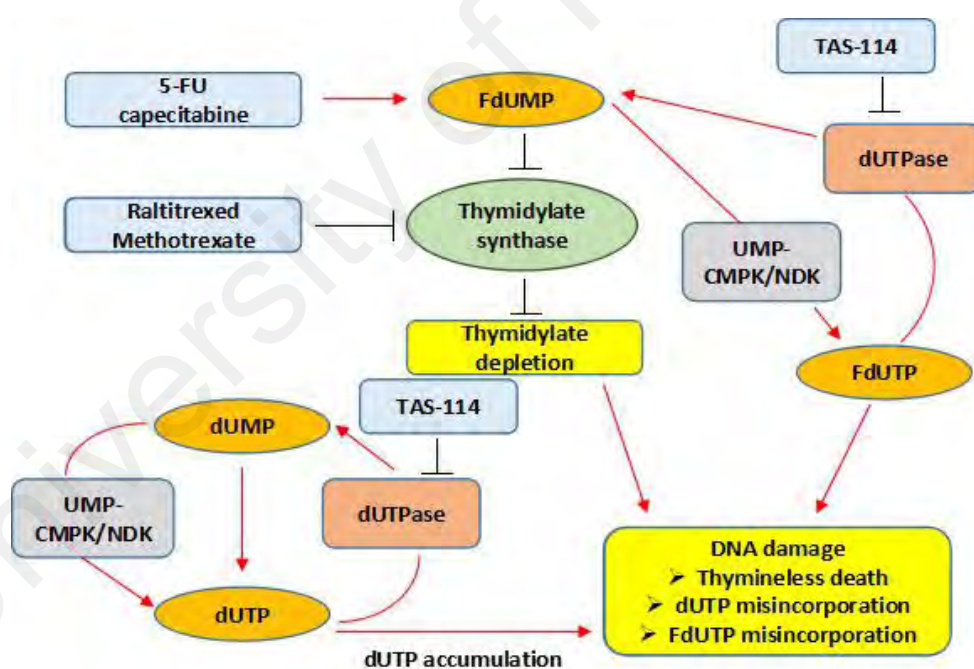


**Figure 2.11: The mechanism of TS inhibition (modified from Wilson et al., 2014).**

The inhibitor of TS can be classified into two major classes; the fluoropyrimidine and antifolate. Fluoropyrimidine-based drug will target nucleotide binding site whilst antifolate will attack folate binding site. Patients with the high level of dihydropyrimide

dehydrogenase activity have to be treated with antifolate, while patients who have defect in the polyglutamylation pathway or in folate transporter should not be treated with antifolates because of metabolic activation (Berger et al., 2004).

#### **2.3.4.1 Fluoropyrimidine-based Drug and Prodrug**

5-FU is a fluoropyrimidine-based drug whilst capecitabine, tegafur-uracil and S-1 are prodrugs. All of them rely on metabolic conversion to 5-FU as their primary mechanism.

##### **a) *5-Fluorouracil (5-FU)***

5-FU has been used to treat colorectal cancer (CRC) and plays the predominant role as the central component of the many effective multidrug treatment regimens used to treat cancer. 5-FU will metabolite to fluorodeoxyuridine monophosphate (FdUMP) that potently inhibits TS. FdUMP and the reduction of folate covalently binds with TS to form ternary complex where cysteine thiol of TS is attached to the 6' position of FdUMP, with the one-carbon group of the folate adjacent to F at the 5' position (Papamichael, 1999).

The bolus and infusional regimens have been compared to identify its toxicity and activity profiles (Cancer et al., 1999). The infusional 5-FU works through TS whilst bolus 5-FU is more likely to work by an action on RNA. In brief, an improvement in survival was reported in infusional 5-FU regimen compared to bolus method (Lamont et al., 1999). The modulation of 5-FU with Leucovorin (LV) has been done to improve its effectiveness by metabolized intracellularly to the reduced folate 5,10-CH<sub>2</sub>THF. Then, elevated levels of this co-factor enhance the formation of a ternary complex between FdUMP, 5,10-CH<sub>2</sub>THF and TS (Cancer et al., 1999).

b) ***Capecitabine***

Capecitabine is an oral anticancer drug converted to 5-FU via a pathway comprising three sequential enzyme reactions that exploit an elevated intratumoral expression of the enzymes (Malet-Martino et al., 2002). Capecitabine is converted to 5'-deoxy-5-fluorocytidine (5'dFCR) by the hepatic enzyme, carboxylesterase. Then, 5'dFCR is converted to 5'-deoxy-5-fluorouridine (5'dFUR) by the enzyme cytidine deaminase, which is expressed in both liver and tumor tissue (Lamont et al., 1999). The final step is the conversion of 5'dFUR to form active metabolite, 5-FU, and is catalyzed by either of the pyrimidine phosphorylase. Capecitabine has lower toxicity profile compared to 5-FU, thus represents an alternative therapeutic option to the patient. In spite of the advantages of capecitabine, it embarks inferior survival rate based on clinical study presented in 2005 (Yun et al., 2010).

**2.3.4.2 Antifolate Drug**

a) ***Raltitrexed***

Raltitrexed (Tomudex) is a quinazoline analog that promises potential to inhibit TS and DHFR. The discovery of this antifolate drug provided depth understanding of the relationship between toxicity and the molecular structure of a compound in the drug discovery, enabling the synthesis of the novel agents with manageable toxicity profiles while retaining potency for anti-tumor activity. It undergoes rapid polyglutamation by the enzyme FPGS and transported into cells via the folate transporter (FOLT) (Jackman et al., 1991). In fact, raltitrexed inhibits TS specifically without requiring any other modulating agent and as an analog of the 5,10-CH<sub>2</sub>THF cofactor, its mechanism of action is not complicated by the multiple outcomes of DNA and RNA incorporation. Besides, it has a manageable toxicity profile while retaining similar clinical effectiveness compared to 5-FU (Ward et al., 1992).

### 2.3.4.3 Combination Therapies

#### a) *5-FU plus oxaliplatin and irinotecan*

The synergetic interaction observed between 5-FU and DNA is persuade to an idea for the combination of 5-FU and folinic acid with oxaliplatin (platinum-based DNA-crosslinking chemotherapeutic agent), with trade name as FOLFOX (Douillard et al., 2010). Then, the combination of 5-FU and folinic acid with irinotecan (an inhibitor of topoisomerase 1) are clinically evaluated and known as FOLFIRI. These triple-drug therapies are frequently administered along with EGFR-targeted antibodies, currently used to treat advanced CRC and high- risk disease patient (Van Cutsem et al., 2011; Douillard et al., 2010).

#### b) *Raltitrexed plus 5-FU*

A summary of phase I and II trials revealed that the combination of raltitrexed with 5-FU provided promising results with favorable response rate. As there are different mechanism pathway and specific target of the binding site, the interaction in the complex may be very complex. However, synergetic cytotoxicity was observed since raltitrexed leads to an increase of intracellular phosphoribosyl pyrophosphate (PRPD) caused by the increase of 5-FU nucleotides formation. Thus, it will enhance the incorporation of 5-FU nucleotides into RNA and increase cell killing (Gorlick et al., 1998).

## 2.4 Computational Approach in Drug Design

Computational approach plays a vital role in drug discovery and development, especially in the pharmaceutical industry. Nowadays, a computational medicinal chemist can explore, develop and optimize the biologically active compounds by software and resources in the computer-aided drug design (CADD) field. In fact, CADD provides beneficial insights into an experimental finding and mechanism of action,

suggestion for synthesis of a new compound and assist to make a cost-effective decision. This platform provides a new hope to the pharmaceutical industry to solve drug issues where numerous compounds discovered using the CADD approach have reached the level of clinical studies or even have succeeded gaining US FDA approval (Talele et al., 2010).

#### **2.4.1 Protein-Ligand System**

Protein-ligand interactions have significant role for the living system. Inhibitors, activators, agonist-antagonist or substrate analogs are known as the ligands and they can be identified by using conventional hit-identifying methods such as the high-throughput screening (HTS) assays or employing various CADD methods. HTS and CADD techniques are complementary to each other in the drug discovery (Ferreire et al., 2010). CADD techniques can optimize the ligands to enhance binding affinity with acceptable pharmacokinetics properties.

In fact, it is more economical and easier to set up than the HTS (Liao et al., 2011). Over past three decades, modeling and prediction of the protein-ligand interactions have been extensively established. Three approaches that are widely used for protein-ligand interaction predictions, which are docking and scoring method, MM-PBSA/GBSA method and free energy calculations method (Mobley et al., 2009). These methods are listed in increasing order of the accuracy and computational demand.

#### **2.4.2 Molecular Docking**

In general, a set of poses for a ligand that can fit into the binding site will be generated by docking and scoring method. Molecular docking is the successful method to predict the binding mode of small molecule like drug candidate to a receptor (Ge et al., 2012). In brief, molecular docking is an automated computer algorithm that attempts to mimic the process of bringing together a protein and a ligand to form a noncovalent

complex via the lowest energy pathway and to reveal the electrostatic and steric complementarity between protein and ligands. The theoretical aspect of docking algorithm is based on Figure 2.12.

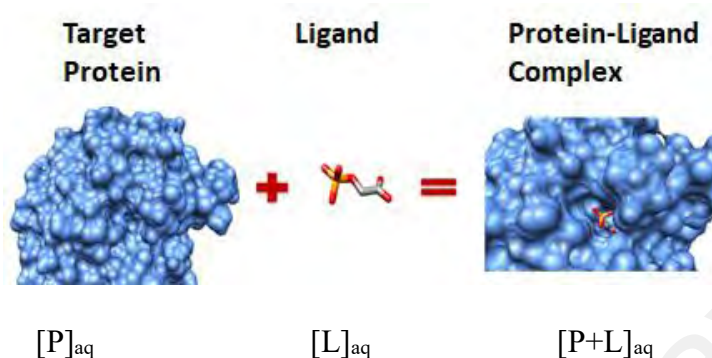
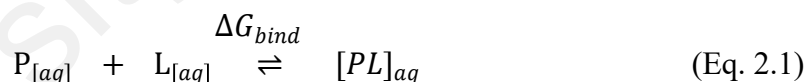


**Figure 2.12: The illustration of molecular docking for protein-ligand system (modified from Alejandra et al., 2013).**

For protein (P) and ligand (L), docking aims at correcting prediction of complex structures  $[P+L]$  under equilibrium conditions (Equation 2.1).



In general, the dissociation constant,  $K_D$  for this reaction is described as :

$$K_D = \frac{[PL]}{[P][L]} \quad (\text{Eq. 2.2})$$

The reciprocal of  $K_D$  or the association constant,  $K_A$  can be used.  $K_D$  is a measure of the affinity of the ligands towards binding site and is measured in molar units, M. If the ligand binding to a single site and not affected by another site of receptor, the value of  $K_D$  indicates the concentration of the ligand whereby half of the binding sites are saturated (Dunn, 2001). A change in binding free energy ( $\Delta G$ ) is influenced by two quantities, which are enthalpy ( $\Delta H$ ) and entropy ( $\Delta S$ ). Enthalpy ( $\Delta H$ ) is the heat of

content whilst entropy ( $\Delta S$ ) is the temperature-independent degree of disorder. The relationship between them is summarized as Equation 2.3 below:

$$\Delta G = \Delta H - T\Delta S \quad (\text{Eq. 2.3})$$

When considering these two quantities, the following factors such as electrostatic and van der Waals interactions, ionization effects, conformational changes and the role of solvents influence the changes in the binding free energy (Perozzo et al., 2004). The binding free energy ( $\Delta G$ ) is related to the binding affinity by Equation 2.4:

$$\Delta G = -RT \ln K \quad (\text{Eq. 2.4})$$

For reaction to occur spontaneously, the change of free energy should be negative. Based on Equation 2.4,  $\Delta G$  is related to an equilibrium constant where  $R$  is a gas constant and  $T$  is an absolute temperature. The  $\Delta G$  can be derived from experimentally measurable quantity,  $K_D$  due to this relation. Biological  $K_D$  values exhibit a wide range from weak to very strong binding depends on the type of inhibitor. Since drug can have side effect due to off-target interaction, very low  $K_D$  value (range of 0.1 to 10 nM) is desired in the drug design (Dunn, 2001).

For this research, the force-field-based scoring functions using molecular mechanics force field such as CHARMM has been used to calculate the enthalpy of binding (Brooks et al., 2009). Usually, the values of non-bonded energy terms are pre-calculated on a grid and then interpolated to the positions where atoms in docked protein-ligand are located. The non-bonded terms including van der Waals (vdW) forces, electrostatic interactions and internal energy components are related to bond length, bond angles and torsional angles. The force-field containing parameters are adjusted to reproduce experimentally or quantum-mechanically determined target data (MacKerell, 2001).

### 2.4.3 Molecular Dynamics Simulation

Molecular dynamic (MD) approaches have been extensively used to resolve motion and interaction as a function of time problem. MD simulation is a powerful tool for studying the binding mechanism at atomic level in the presence of explicit solvent (LeszczynskiJerzy, 2005) and characterize the protein flexibility (Mobley et al., 2009). It has been used to monitor the time-dependent processes of molecules by solving an equation of motion. Different molecular dynamic approaches involve different equation of motion that can be used depending on the aim of the simulation (Becker & Watanabe, 2001).

Particle Mesh Ewald summation (PME) method allows all atom simulation to be immersed in the explicit water (Freddolino et al., 2006). The accuracy and computational efficiency of the simulation depends on the time step,  $\Delta t$ . A short time step will increase the accuracy of the simulation, whereas a longer time step will allow sampling of a wider phase space with being small relative to the period of the fastest motion in the structure. In fact, bonds between hydrogen and heavy atoms are the fastest to move (Becker & Watanabe, 2001). In addition, time step also affects the stability of the system in MD simulation since a large time step allows more fluctuation of the system energy (van Gunsteren & Berendsen, 1977).

#### 2.4.3.1 General Amber Force Field (GAFF)

Molecular mechanics force field is a key component that gives significant impact in the investigation of the protein-ligand structure for rational drug design (Kollman & Case, 2004). Since AMBER force field has limited parameters for the organic molecules, general amber force field (GAFF) is more suitable for drug design and protein-ligand interactions. GAFF is compatible with existing Amber force field for proteins and nucleic acids, and has parameter for most of the organic molecules that consist of H, C,

N, O, S, P, and halogens. The force constant and partial atomic charges can be estimated from both empirical and heuristic models (Wang et al., 2004). Similar with AMBER, the restrained electrostatic potential (RESP) at HF/6-31G\* is the default charge approach applied in GAFF parameterization (Bayly et al., 1993).

#### 2.4.3.2 Molecular Mechanics/ Poisson-Boltzmann Surface Area (MM-PBSA) and Molecular Mechanics/Generalized Born Surface Area (MM-GBSA).

The relative binding affinity of ligand to the target protein can be reproduced with good accuracy and less computational effort by using Molecular Mechanics/ Poisson-Boltzmann Surface Area (MM-PBSA) and Molecular Mechanics/Generalized Born Surface Area (MM-GBSA). In fact, the free energies can be decomposed into insightful interactions and desolvation components (Archontis et al., 2001).

Both Poisson-Boltzmann (PB) and Generalized Born (GB) approaches calculate the binding free energy of protein-ligand complex by the following equations:

$$\Delta G_{\text{bind}} = G_{\text{com}} - (G_{\text{rec}} + G_{\text{lig}}) \quad (\text{Eq. 2.5})$$

$$\Delta G_{\text{bind}} = \Delta H - T\Delta S \approx \Delta E_{\text{MM}} + G_{\text{sol}} - T\Delta S \quad (\text{Eq. 2.6})$$

$$\Delta E_{\text{MM}} = \Delta E_{\text{internal}} + (\Delta E_{\text{internal}} + \Delta E_{\text{vdw}}) \quad (\text{Eq. 2.7})$$

$$\Delta G_{\text{sol}} = \Delta G_{\text{PB/GB}} + G_{\text{SA}} \quad (\text{Eq. 2.8})$$

where  $\Delta G_{\text{bind}}$  refer to the binding free energy of protein-ligand complex whilst  $G_{\text{com}}$ ,  $G_{\text{rec}}$  and  $G_{\text{lig}}$  represent the free energy of complex, protein and ligands, respectively. Basically, total free energy consist of enthalpy ( $\Delta H$ ) which is composed of the enthalpy changes in the gas phase upon complex formation ( $\Delta E_{\text{MM}}$ ) and the desolvation free energy ( $\Delta G_{\text{sol}}$ ), and the conformational entropy ( $T\Delta S$ ) upon association of ligands.  $\Delta E_{\text{MM}}$  is the summation of internal energy term ( $\Delta E_{\text{internal}}$ , composed of bond, angle and

dihedral energies), the electrostatic energy ( $\Delta E_{\text{electrostatic}}$ ) and van der Waals energy ( $\Delta E_{\text{vdw}}$ ) between protein and ligands.  $\Delta G_{\text{sol}}$  is the summation of the electrostatic ( $\Delta G_{\text{PB/GB}}$ ) and non-polar contribution ( $\Delta G_{\text{SA}}$ ) (Hou et al., 2011).

Nevertheless, they are differences in terms of the desolvation energy calculation, where the polar contribution of desolvation is computed by implicit solvation of PB models for the PBSA approach whilst GB model for the GBSA approach. Even though PB employs a more rigorous algorithm, but GB model also has an advantage since its parameters have been optimized by fitting experimental data and both models performance depend on the system (Onufriev et al., 2004).

#### **2.4.4 2D Quantitative Structure- Activity Relationship (2D QSAR)**

Quantitative structure-activity relationship (QSAR) modelling is a key to predict physicochemical properties and rationalizing experimental binding data or inhibitory activity of the chemical compounds. The 2D QSAR is a conceptual way of finding a simple equation that is valuable to predict some property from the molecular structure of a compound. It is including correlation (model) between a set of independent variables (chemical descriptors) calculated from the chemical graphs, and the dependent variables such as binding affinity, log P, or the pKa value to predict the properties of potential compound (Sproun et al., 2010). Hence, it becomes an important tool for predicting drug-like organic compounds and widely employed in the field of absorption, distribution, metabolism, elimination and toxicity (ADMET prediction) (Liao et al., 2011).

##### **2.4.4.1 Lipinski's Rule of Five**

Drug-likeness analyses have been widely used across the pharmaceutical industry to indicate the potential of a molecule to become a drug. The Lipinski's 'rule of five' and lead-likeness 'rule of three' are the benchmark to understand the drug-likeness in drug

and lead discovery evolution. Compounds derived from the majority of known drugs and conforming to these rules have the potential to exhibit drug-like behavior. As implemented in Lipinski's 'rule of five', the compounds have possible absorption and permeability problems if any two of the following conditions are satisfied (Lipinski et al., 1997):

- Molecular weight > 500
- Number of hydrogen bond acceptors > 10
- Number of hydrogen bond donors > 5
- Calculated log P > 5.0 for ClogP or > 4.15 for MlogP

Hydrogen bond acceptors are referring to oxygen (O) and nitrogen (N) atoms whilst N-H or O-H is considered as hydrogen bond donors. Here, Log P is defined as the octanol/water partition coefficient of a compound to measure the lipophilicity.

#### **2.4.4.2 Absorption, Distribution, Metabolism, Elimination and Toxicity (ADMET) Prediction.**

The efficacy, safety, and cost-benefit are critical factors that contribute to the decision-making drug process (Oprea et al., 2011). Thus, ADMET parameters are significant for the drug candidates in order to reduce late-stage failure and minimize cost (Wang et al., 2009). *In silico* ADMET prediction programs are capable to predict the potential of ADME/T risks that provide great benefit to the medicinal chemists (Gleeson et al., 2011). The right combination of statistical techniques, molecular descriptors, validation method, and experimental data used are the significant factors that influence the quality of ADMET models (Egan et al., 2007).

#### **2.4.5 Factors Affecting Protein-Ligand Binding Affinity**

The binding affinity strength of protein-ligands is contributed from the non-covalent interactions, entropy, desolvation, the flexibility of receptor structure and the structural

water molecules in the binding site (Gohlke & Klebe, 2002). The electrostatic interactions and van der Waals forces are non-covalent interactions that play the major role in the complex.

#### 2.4.5.1 Non-Covalent Interactions

##### a) *Electrostatic Interaction*

Briefly, the two oppositely charged particles are electrostatically attracted to each other to achieve a minimum energy. The predominant type of electrostatic interaction which is vital for the protein-ligand complex formation including salt bridges, hydrogen bond, and metal interactions are illustrated in Figure 2.13 (Gohlke & Klebe, 2002; Bleicher et al., 2003). Salt bridge is formed when there is close interaction between two oppositely charged amino acid residues and often involve hydrogen bonding in addition to electrostatic interaction (Kumar & Nussinov, 2002).

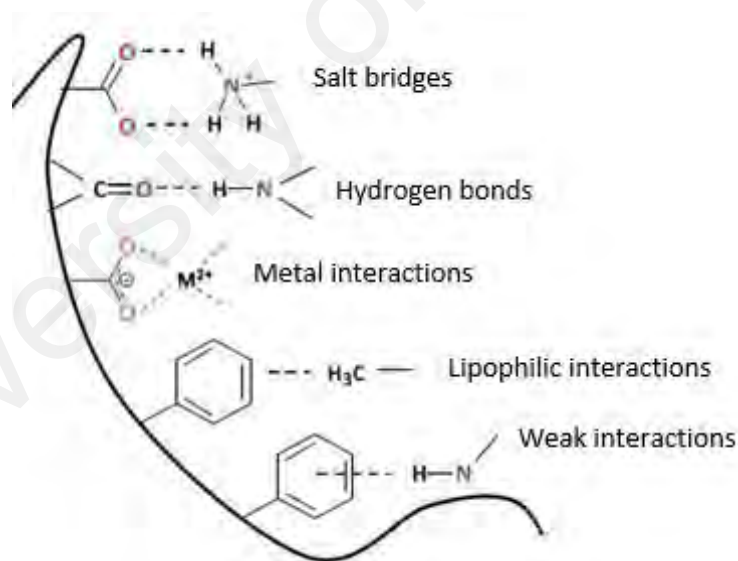


**Figure 2.13: The predominant types of non-bonded interaction in the protein-complex (modified from Bleicher et al, 2003).**

Meanwhile, hydrogen bonding occurs between two electronegative atoms, where one of them has a covalently bound hydrogen atom (donor) whilst the other has a lone pair of electrons (acceptors). It is considerably weaker than typical covalent bond but pivotal

to enhance the stability of protein structure (Hubbard et al., 2010). It is considered as strong and energetically favorable hydrogen bond if the donor-acceptor separation  $\leq 3.5$  Å, hydrogen-acceptor distance  $\leq 2.5$  Å with angle is close to  $180^\circ$  (McDonald & Thornton, 1994).

#### **b) *Van der Waals (VdW) Force***

Van der Waals force occurs when there is an attractive (London force) and repulsive force between non-bonded atoms. London force is caused by transient polarization of the non-polar particles that allows a particle with a momentary low electron density to be attracted towards a particle with a momentary high electron density. Repulsive force is originated from Pauli extension principle where two electrons cannot occupy the same quantum state simultaneously causing interaction energy to increase abruptly when two particles are close enough to penetrate the electron shell of another (Burgoyne, 2006).

#### **c) *Hydrophobic Interactions***

Hydrophobic interaction involves contact between non-polar parts of the molecule and entropy-driven that plays a significant role in the ligand binding. Non-polar parts at the interacting surface are buried upon binding causes displacement of the water molecules, hence increasing the entropy (Bleicher, 2003).

#### **d) *Aromatic-aromatic and Aliphatic-aromatic Interactions***

Aromatic rings interact with each other by the T-shaped edge to face or parallel displaced stacking interaction. However, parallel-displaced geometry has been often observed in the protein structures (McGaughey et al., 1998). Meanwhile, edge-to-face

and parallel-displaced interactions of aliphatic-aromatic interaction usually occur at the non-polar interfaces (Bissantz et al., 2010).

#### **2.4.5.2 Desolvation**

Since water acts as a medium in the protein-ligand complex, thus the dynamic hydrogen bond network of water contributes to the interactions in complex. Nevertheless, the transfer molecules cause disruption of this network and re-organization of water molecules, hence resulting unfavorable loss of the entropy (Gohlke & Klebe, 2002; Bissantz et al., 2010; Bleicher, 2003). An unfavorable desolvation of the binding site causes in full or partial loss of the affinity (Bleicher, 2003).

#### **2.4.5.3 Flexibility of Receptor**

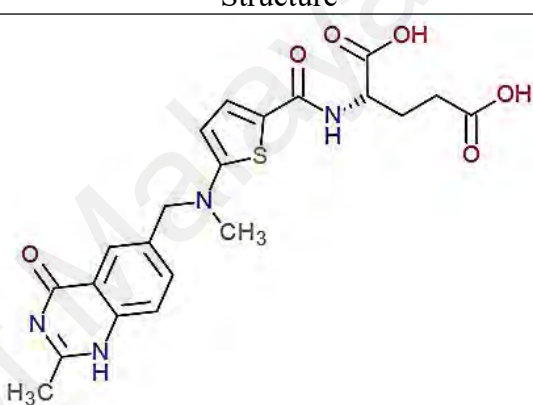


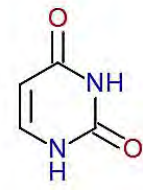
The conformational flexibility of protein is a pivotal issue in the molecular recognition. Upon the ligand binding, protein-binding sites exhibit a variety motion in the rearrangement of the small scale side chain to loop movement in the binding site. Previous studies reveal that the different ligands result different conformational change of the receptor (Huth et al., 2007; Brough et al., 2009).

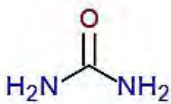
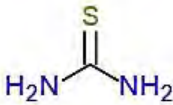
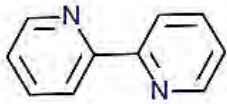
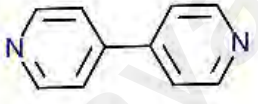
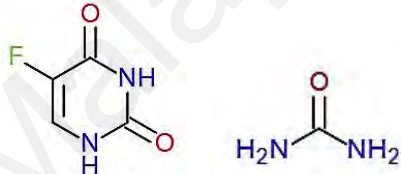


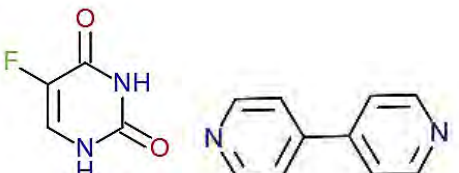
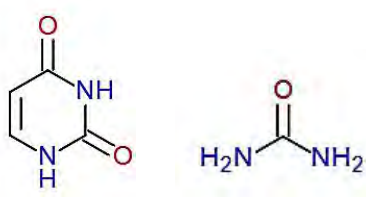
## CHAPTER 3: METHODOLOGY

### 3.1 The Classification of Ligands.

All the ligands have been classified into five systems to see their potential for the TS inhibition (Table 3.1).

**Table 3.1: The system of ligands.**

Systems	Ligand	Structure
Antifolate	Raltitrexed	
Reference ligand	dUMP	
Active Pharmaceutical Ingredients (API)	5-Fluorouracil (5-FU)	
	Uracil	

Conformer	Urea	
	Thiourea	
	2,2'-bipyridine	
	4,4'-bipyridine	
Co-crystals	5-Fluorouracil-urea (5FU-U)	
	5-Fluorouracil-thiourea (5FU-TU)	
	5-Fluorouracil-2,2'-bipyridine (5FU-22)	
	5-Fluorouracil-4,4'-bipyridine (5FU-44)	
	Uracil-urea (UU)	

## **3.2 The Potential of Co-crystal as Anti-cancer Inhibitor**

### **3.2.1 Molecular Docking Studies of Protein-Ligand Systems**

The PDB file of thymidylate synthase (PDB ID: 1HVY) with 1.9 Å resolution was obtained from the RCSB protein data bank (<http://www.pdb.org>). 1HVY is the closed conformation of recombinant hTS complex with dUMP and in the presence of raltitrexed (Tomudex, ZD1694), as an antifolate drug (Phan et al., 2001). Uracil and 5-fluorouracil were active pharmaceutical ingredients (API) whilst urea, thiourea, 2, 2-bipyridine and 4, 4-bipyridine were conformers that need to form dual co-crystal drugs. All of them were optimized by employing DFT method with B3LYP/6-311G\*\* (Axel, 1993; Lee et al., 1988) in Gaussian09 program (Version 09; Frisch, 2009). The docking procedure of dUMP (reference ligand), API, conformer and a series of co-crystal were conducted by using CDOCKER protocol that implemented in the receptor-ligand interaction of Discovery Studio Client 2.5. (Version 2.5; Accelrys Software Inc, 2007).

CDOCKER is a grid-based molecular docking method that employs CHARMM. The protein and all the ligands were pretreated and minimized by applying Memony Rone partial charged (Memony & Rone, 1992). Hydrogen atoms were added to the structure and all ionisable residues were set at their default protonation state at a neutral pH. By using CDOCKER, the receptor is held rigid while the ligands are allowed to flex during the refinement. The translating center of the ligand to a specified position within the active site of the protein produces a series of random rotations. Thus, random orientations of the conformation are generated.

Each orientation was made accountable to simulate annealing molecular dynamics involving heating on high temperature of 700 K in 2000 steps and cooling down to 300 K in 5000 steps. Since the ligands are fluoropyrimidine-based TS inhibitor, the site sphere was selected according to the binding location of dUMP ligand in nucleotide

binding site with the radius of 20 Å (Phan et al., 2001). Fifty poses were sorted for each ligand based on CHARMM energy and the complex structure was selected based on the CDOCKER interaction energy. The highest –CDOCKER interaction energy express the best pose of each ligand (Dai et al., 2010).

Protein-Ligand Interaction Profiler (PLIP) server (Salentin et al., 2015) for the dUMP, the best of API and conformer, and all the co-crystals determined the interaction of protein-ligand complex. The binding energy of the complex was calculated by using the binding energies protocol (Version 2.5; Accelrys Software Inc, 2007). It can estimate the binding energy between the target protein and ligand. In order to acquire the binding energy, the best poses of each ligands were sort out based on Equation 3.1:

$$Energy_{Binding} = Energy_{Complex} - Energy_{Ligand} - Energy_{Receptor} \quad (Eq. 3.1)$$

### 3.2.2 Molecular Dynamics of Protein-Ligand Complexes.

The best co-crystal (5FU-U) and dUMP complexes were further analysed by the molecular dynamic simulation to verify its stability. Deriving atomic charges of the 5FU-U co-crystal, dUMP and tomudex were performed by R.E.D Tools (RESP and ESP charge derive, <http://q4md-forcefieldtools.org/RED/>) (Vanquelef et al., 2011). Different quantum mechanical programs were employed for the geometry optimization. In this study, RESP program was used to perform charge fitting suitable for molecular dynamics simulation. Charge values are reproduced by defining the tight optimization criteria and controlling the molecular orientation of each optimization geometry (Dupradeau, 2010). For the preparation of ligands, the general AMBER force field (GAFF) was applied by using antechamber module (Wang et al., 2004).

Molecular dynamics (MD) simulation at the molecular mechanics level was employed using ff12SB (Salomon-Ferrer et al., 2013) force field as implemented in

AMBER12 (Case et al., 2012) suite of programs to describe the molecular characteristics of the complex. PROPKA program had been used to assign the ionization state of an amino acid with electrically charged side chain (Li et al., 2005). The complexes were solvated in a cubic box of TIP3PBOX (Jorgensen, 1983) water extending at 12 Å in each direction from the solute with Na<sup>+</sup> ions added as the neutralizing counterions. To compute the non-bonded interactions, the cut-off distance was kept to 10 Å.

All simulations were performed under the periodic boundary conditions (Essman et al., 1995) and the long-range electrostatic were treated by applying particle-mesh-Ewald method (Kollman et al., 2000; Hou et al., 2011). The energy minimization and molecular dynamics (MD) simulations were performed using PMEMD.CUDA (Goetz et al., 2012; Grand et al., 2013) from AMBER12 on graphical processors (GPUs) Quadro 2000D produced by NVIDIA which speed up simulation wall time required to obtain trajectory file for each simulation. Initially, the temperature of each system was increased gradually from 0 to 310 K over a period of 60 ps of NVT dynamics. This was followed by 300 ps of NPT equilibration at 310.15 K and 1 atm pressure and then 75ns of NPT-MD simulation was performed for properties collection.

The structural properties and intermolecular interaction of the protein-ligand complexes were analyzed within 75 ns of MD trajectories to identify their stability for the long run simulations. The trajectories were analyzed using PTRAJ module of the amber package. The root mean square deviation (RMSD) was used for verification of the system stability.

### **3.2.3 Binding Free Energy Calculation and Per-residue Free Energy Decomposition**

The calculation and decomposition of binding free energy of the complexes were evaluated based on the Molecular Mechanics/Poisson-Boltzmann Surface Area (MM/PBSA) and Molecular Mechanics/Generalized Born Surface Area (MM/GBSA) protocol implemented in AMBER12 to estimate the binding affinity between target protein (TS) and ligands (Gilson et al., 1998; Wang et al., 2001).

Five hundred MD snapshot were extracted from the last 5 ns trajectories simulation and were used as a structural ensemble to evaluate the MM-PBSA/GBSA binding free energies. They were computed by Amber SANDER module (Kollman et al., 2000). Then, the per-residue free energy decomposition was conducted to obtain free energy that contributes to the specific binding. This approach calculates the energy contribution of single residues by summing its interaction with all residues in the system, which possible for molecular mechanics and free energy solvation (Gohlke et al., 2003).

## **3.3 Modification to Enhance Potential of Co-crystal to Inhibit TS**

### **3.3.1 Fragment Linking Approach**

The best co-crystal (5FU-U co-crystal) was modified by fragment linking approach as Figure 3.1 to enhance its stability and binding interaction. It was structurally connected through heptyl group to mimic the reference ligand (dUMP). The rotatable bonds greater than 10 will decrease oral bioavailability (Veber et al., 2002). The compound 1 was optimized by employing DFT method with B3LYP/6-311G\*\* (Axel, 1993; Lee et al., 1988) in Gaussian09 program (Version 09; Frisch, 2009). The optimized geometry was further used for docking study.

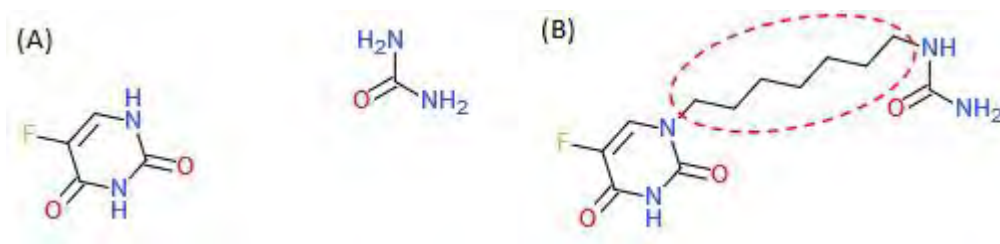


**Figure 3.1: The structures of (A) 5FU-U co-crystal and (B) compound 1.**

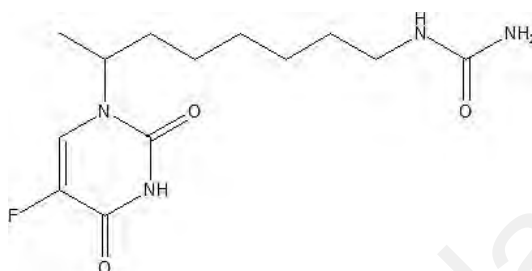


**Figure 3.2: The 2D structure of compound 1.**

### 3.3.2 Molecular Docking Study

The docking procedure of modified co-crystal (compound 1) with raltitrexed was conducted by using similar CDOCKER protocol as dUMP and co-crystal complexes (Version 2.5; Accelrys Software Inc, 2007). The protein and ligand were pretreated and minimized by applying Momany Rone partially charged (Momany & Rone, 1992) and CHARMM force field. Hydrogen atoms were added to the structure and all ionisable residues were set at their default protonation state at a neutral pH.

Each orientation was made accountable to the simulated annealing molecular dynamics involving the heating up to the high temperature of 700 K in 2000 steps and cooling down to 300K in 5000 steps. The site sphere was selected according to the binding location of dUMP ligand in nucleotide binding site with radius of 20 Å (Phan et al., 2001). Fifty poses were sorted for each ligand based on CHARMM energy and the complex structure was selected based on the CDOCKER interaction energy. The lowest CDOCKER interaction energy expresses the best pose of each ligand (Dai et al., 2010).

### 3.3.3 Molecular Dynamic Simulation

The method of molecular dynamic study for compound 1 is standardized with 5FU-U co-crystal and dUMP complexes. Deriving atomic charges of compound 1 and raltitrexed were performed by R.E.D Tools (RESP and ESP charge derive, <http://q4md-forcefieldtools.org/RED/>) (Vanquelef et al., 2011). For the preparation of ligands, the general AMBER force field (GAFF) was applied by using antechamber module (Wang et al., 2004).

Molecular dynamics (MD) simulation at the molecular mechanics level was employed using ff12SB (Salomon-Ferrer et al., 2013) force field as implemented in AMBER12 (Case et al., 2012) and PROPKA program has been used to assign the ionization state of amino acid with electrical charged side chain (Li et al., 2005). The complex was solvated in a cubic box of TIP3PBOX (Jorgensen, 1983) water extending at 12 Å in each direction from the solute with Na<sup>+</sup> ions were added as the neutralizing counterions. To compute the non-bonded interactions, the cut-off distance Na<sup>+</sup> ions added as the neutralizing counterions. To compute the non-bonded interactions, the cut-off distance was at 10 Å.

All simulations were performed under periodic boundary conditions (Essman et al., 1995) and long-range electrostatic were treated by applying particle-mesh-Ewald method (Kollman et al., 2000; Hou et al., 2011). Energy minimization and molecular dynamics (MD) simulations were performed by using PMEMD.CUDA (Götz et al., 2012; Grand et al., 2013) from AMBER12 on graphical processors (GPUs) Quadro 2000D produced by NVIDIA which accelerate simulation wall time required to obtain trajectory file for each simulation. The temperature of each system was increased constantly from 0 to 310 K within 60 ps of NVT dynamics. This was proceeded with

300 ps of NPT equilibration at 310.15 K and 1 atm pressure and 75ns of NPT-MD simulation was executed for properties collection.

The system stability and flexibility of protein-ligand complex in the long run simulation was analyzed using PTRAJ module of AMBER package. The structural properties and intermolecular interactions of the protein-ligand complexes were analyzed within 75 ns of MD trajectories and were verified by the root mean square deviation (RMSD).

#### **3.3.4 Binding Free Energy Calculation and Per-residue Free Energy Decomposition**

Five hundred MD snapshot were extracted from the last 5 ns trajectories simulation and used as the structural ensemble to evaluate the MM-PBSA/GBSA binding free energies. They were computed by Amber SANDER module (Kollman et al., 2000). Further, the per-residue free energy decomposition was carried out to obtain free energy that contributes to the specific binding. This approach calculates the energy contribution of single residues by summing its interaction with all residues in the system, which is possible for molecular mechanics and free energy solvation (Gohlke et al., 2003).

#### **3.4 Insight into Protein-Ligand Interaction**

The interaction of protein-ligand complexes at 75 ns was determined by Protein-Ligand Interaction Profiler (PLIP) server (<https://projects.biotec.tu-dresden.de/plip-web>), a novel web service for fully automated detection and visualization of the relevant non-covalent protein-ligands contacts in 3D structures (Salentin et al., 2015). The intermolecular hydrogen bonds formation between protein and ligand were evaluated through PTRAJ module for the last 5 ns trajectory in AMBER12. PyMOL 1.6 (Schrödinger, 2015) generated the high-resolution images.

### **3.5 Drug-likeness Analysis**

#### **3.5.1 Physicochemical Properties Prediction**

The predicted physicochemical properties analysis of the potential ligands was performed by ChemAxon to predict “drug-likeness” ligand. Marvin was used for drawing, displaying and characterizing the chemical structures, substructures, and reactions, Marvin 15.6.8, 2015, ChemAxon (<http://www.chemaxon.com>). In this study, the focus was on the log p, hydrogen donor count, hydrogen acceptor count, molecular weight, polar surface area (PSA) based on the Lipinski’s rule of five (RO5).

#### **3.5.2 2D QSAR by ADMET Prediction**

Computer was aided for the absorption, distribution, metabolism, elimination, and toxicity (ADMET) prediction was evaluated using ADMET descriptors in the Discovery Studio 2.5 (Version 2.5; Accelrys Software Inc, 2007). The ADMET parameters for chemical structure of the ligands are based on the available drugs information. These parameters including ADMET absorption which predicts human intestines absorption (HIA) after oral administration where the absorption level of HIA model are determined by 95% and 99% confidence ellipses in the ADMET\_PSA\_2D, ADMET\_AlogP98 plane (Egan et al., 2000). The ADMET aqueous solubility predicts the solubility of compound at 25 °C based on the genetic partial square method on training set of 784 compounds with experimentally measured solubility (Cheng et al., 2003). Besides, the blood-brain penetration of molecule after oral administration is predicted through ADMET blood brain barrier (BBB) parameter that derived from over 800 compounds that are known to enter central nervous system (CNS) after oral administration (Egan et al., 2000).

ADMET plasma protein binding model predicts the potential of compound to be highly binding with carrier protein in blood. The binding levels were predicted based on

marker similarities that was modified due to conditions on the calculate log P (Dixon et al., 2001). ADMET CYP2D6 binding predicts cytochrome P450 2D6 enzyme inhibition according to the training set of 100 compounds with known CYP2D6 inhibitions (Susnow et al., 2003). ADMET hepatotoxicity will predict the hepatotoxic nature of the compound according to an ensemble recursive partitioning model of 382 training compounds known to exhibit liver toxicity (Cheng et al., 2003).

University of Malaya

## CHAPTER 4: RESULT AND DISCUSSION

### 4.1 The Potential of Co-crystals and Compound 1 as the Cancer Inhibitors

#### 4.1.1 Molecular Docking Study

The potential of ligands as anti-cancer inhibitors in the presence of raltitrexed was evaluated based on CDocker interaction. The combination of raltitrexed with other anti-cancer agents is possible since they are different mechanisms, occupying different binding sites and have different specificities for the enzyme. Since raltitrexed is still in the folate binding site, the possibility of ligands to bind with TS was investigated by targeting nucleotide binding site. Thus, both promising binding sites; nucleotide and folate will be disrupted at the same time. Hence, the activity of thymidylate synthase can be reduced. The overall docking structures and superimpositions of ligands for dUMP complex, co-crystal complexes and compound 1 complex were depicted in Figure 4.1. Due to the observation, 5FU-U co-crystal, 5FU-44 co-crystal, UU co-crystal and compound 1 occupy similar positions to the reference ligand, dUMP.

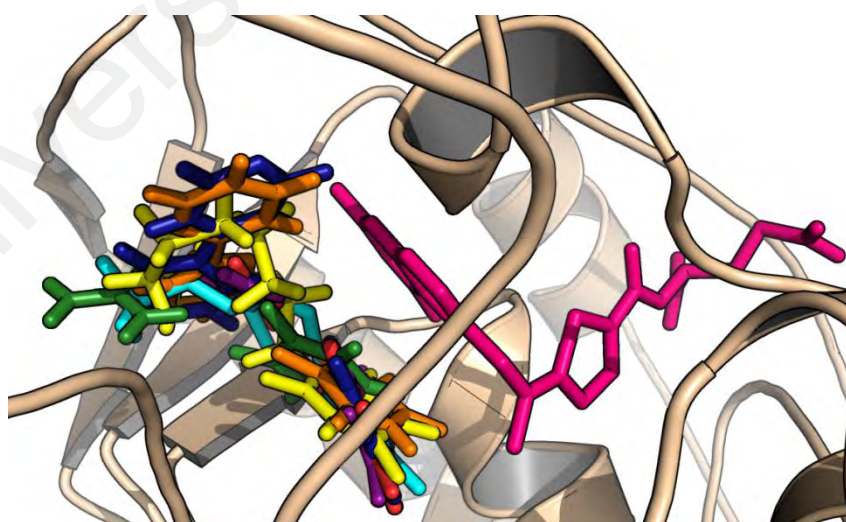


**Figure 4.1:** The overall docking structures and superimpositions of the ligands for all complexes where dUMP (light blue), 5FU-U co-crystal (red), 5FU-TU co-crystal (green), 5FU-22 (orange), 5FU-44 (blue), UU (purple), compound 1 (yellow) and raltitrexed (pink).

The strength of the protein-ligand interactions was analyzed based on CDOCKER interaction to evaluate the best pose of each dock complexes since random conformations were generated by docking. The more negative value for CDOCKER interaction revealed strong binding between the target protein (TS) and ligands. The result of docking for ligands with TS was depicted in Figure 4.2

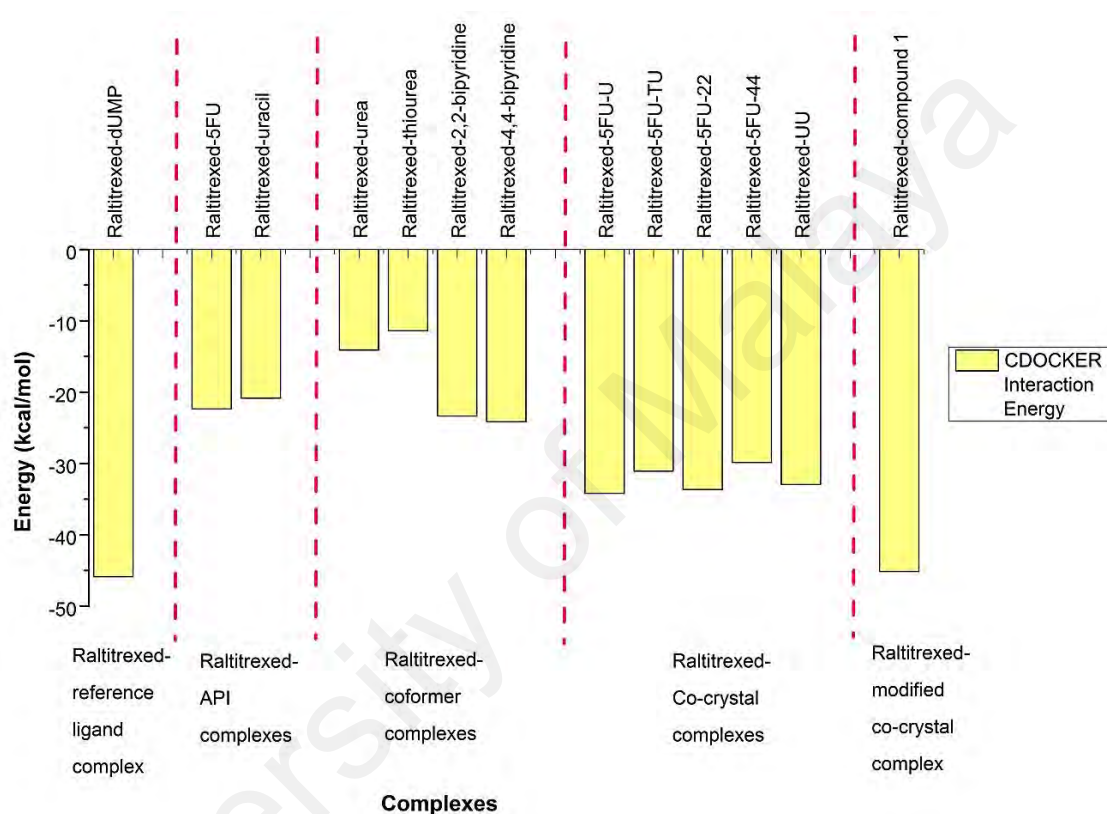


**Figure 4.2: The CDOCKER interaction energy of complexes in kcal/mol.**

As stated on the graph, 5FU-U co-crystal revealed the best interaction with TS among the co-crystals complexes in the presence of raltitrexed. The potential of TS inhibition were increased when the best API, 5FU combined with urea as a dual drug co-crystal (5FU-U) than 5FU alone with -34.22 kcal/mol and -22.38 kcal/mol, respectively. Even 4,4-bypiridine shows the best binding among raltitrexed-conformer complexes (-24.17 kcal/mol), but co-crystallize it with 5FU not given the best result with only -29.88 kcal/mol of cdocker interaction. However, the 5FU-U co-crystal still

cannot enhance the binding affinity of raltitrexed since it has higher interaction energy (-34.2 kcal/mol) than raltitrexed-dUMP complex. In contrast, compound 1 in the presence of raltitrexed has improved the potential to bind well with TS by expressing similar interaction energy (-45.15 kcal/mol) with raltitrexed-dUMP complex (-45.88 kcal/mol).

Insight further into the protein-ligand interactions of docked complexes (Figure 4.3), there are several intermolecular hydrogen bonds formed in the raltitrexed-dUMP complex. Raltitrexed has hydrogen bonding with Gly222A and Asp218A whilst dUMP has hydrogen bonding with Arg215A, Asp218A, Arg176B, Asn226A, and Tyr258A. For co-crystal complexes, raltitrexed-5FU-U co-crystal complex reveals hydrogen bonds between raltitrexed with Gly222A and Asp218A, whilst 5FU-U co-crystal has hydrogen bonding with Gln214A, Arg176B, and Asp218A. Several hydrogen bonds were formed in the raltitrexed-5FU-TU co-crystal complex indicated the significant of Ser216A, Asp218A, Gly222A, Arg175B, and His196A residues in the complex.

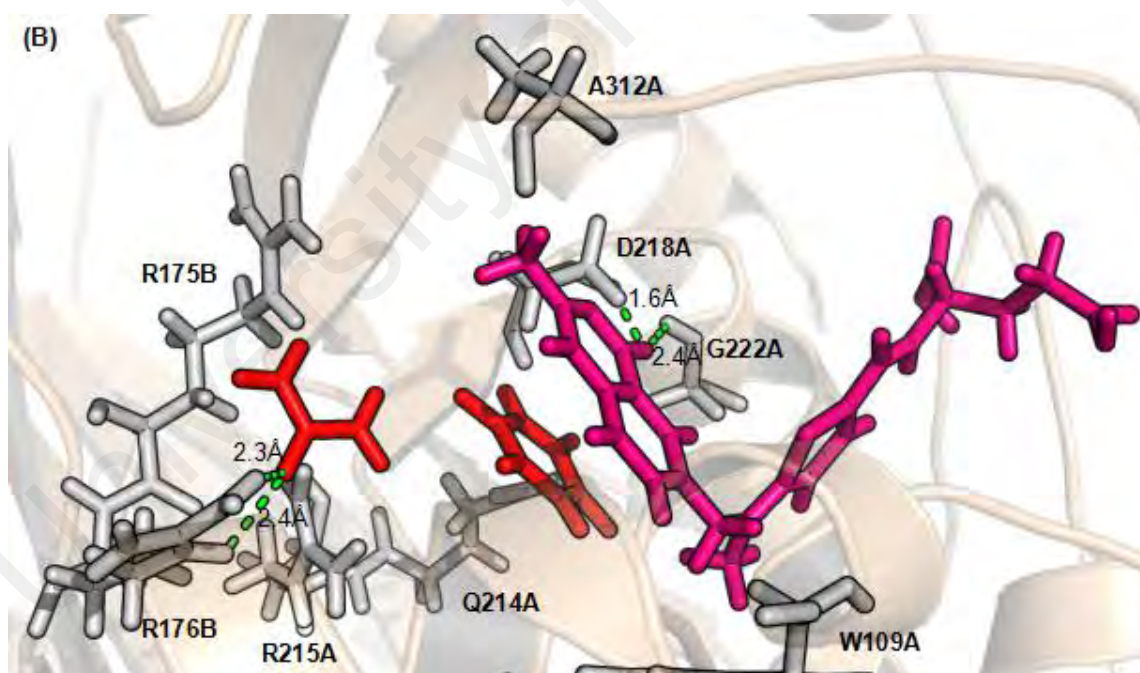
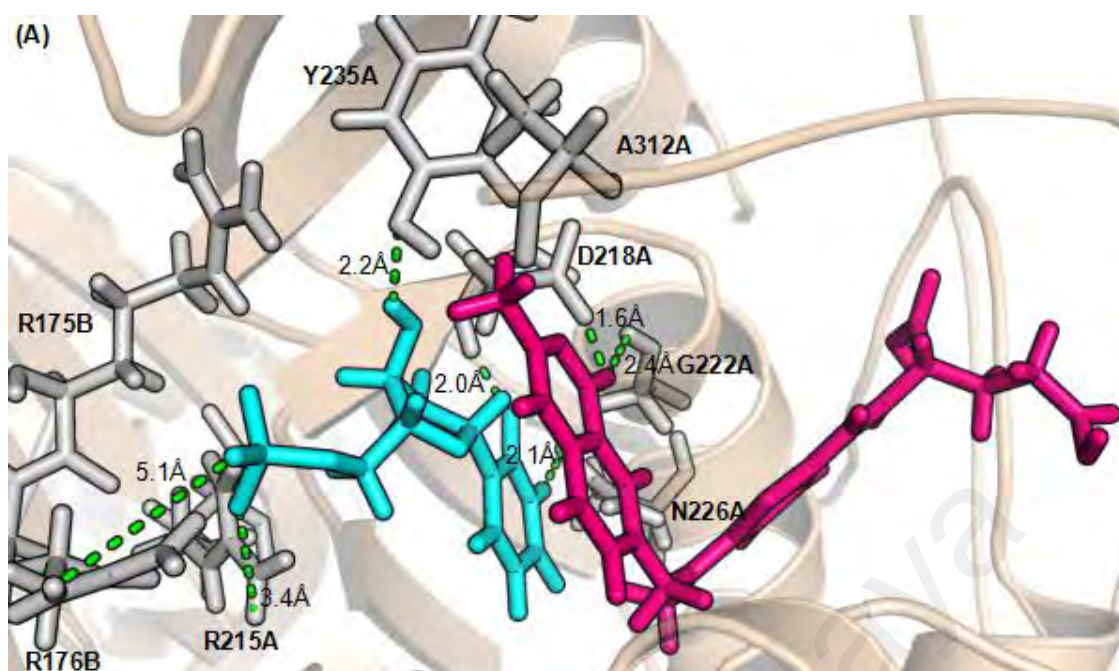


**Figure 4.3:** The intermolecular hydrogen bonds (green dotted line) in the docked complexes where (A) raltitrexed (pink)-dUMP (light blue) complex, (B) raltitrexed-5FU-U co-crystal (red) complex, (C) raltitrexed-5FU-TU co-crystal (green) complex, (D) raltitrexed-5FU-22 co-crystal (orange) complex, (E) raltitrexed-5FU-44 co-crystal (blue) complex, (F) raltitrexed-UU co-crystal (purple) complex and (G) raltitrexed-compound 1 (yellow) complex.

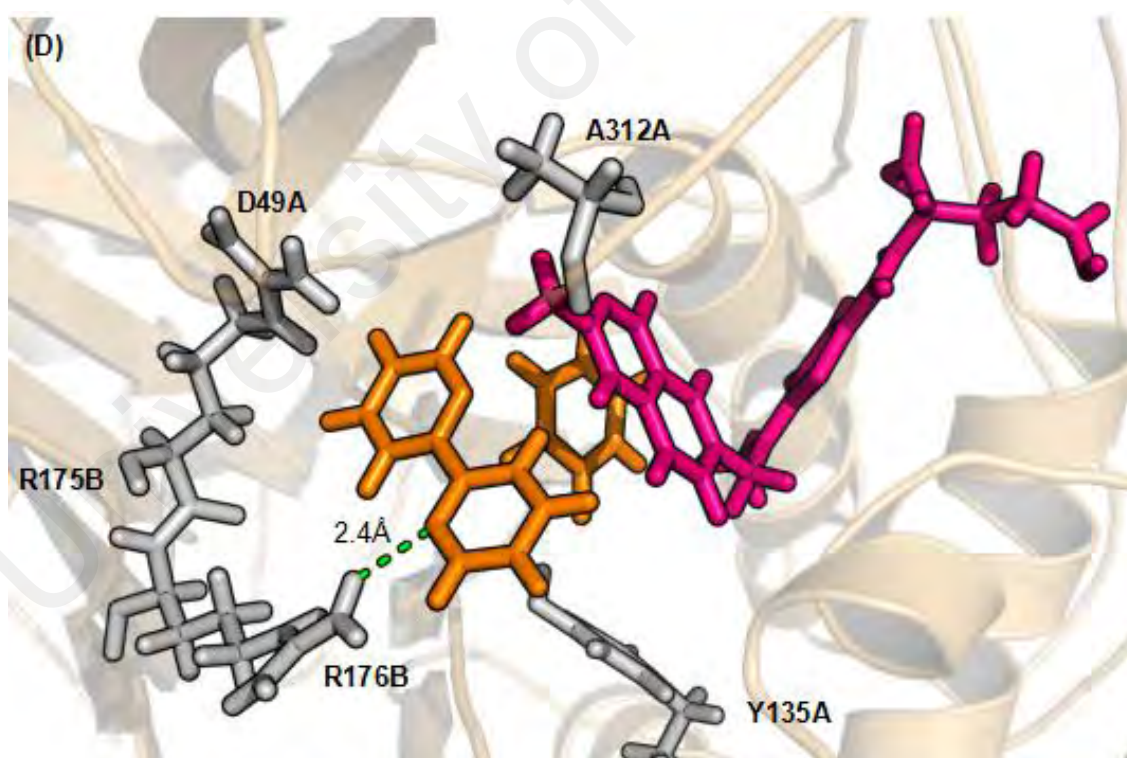
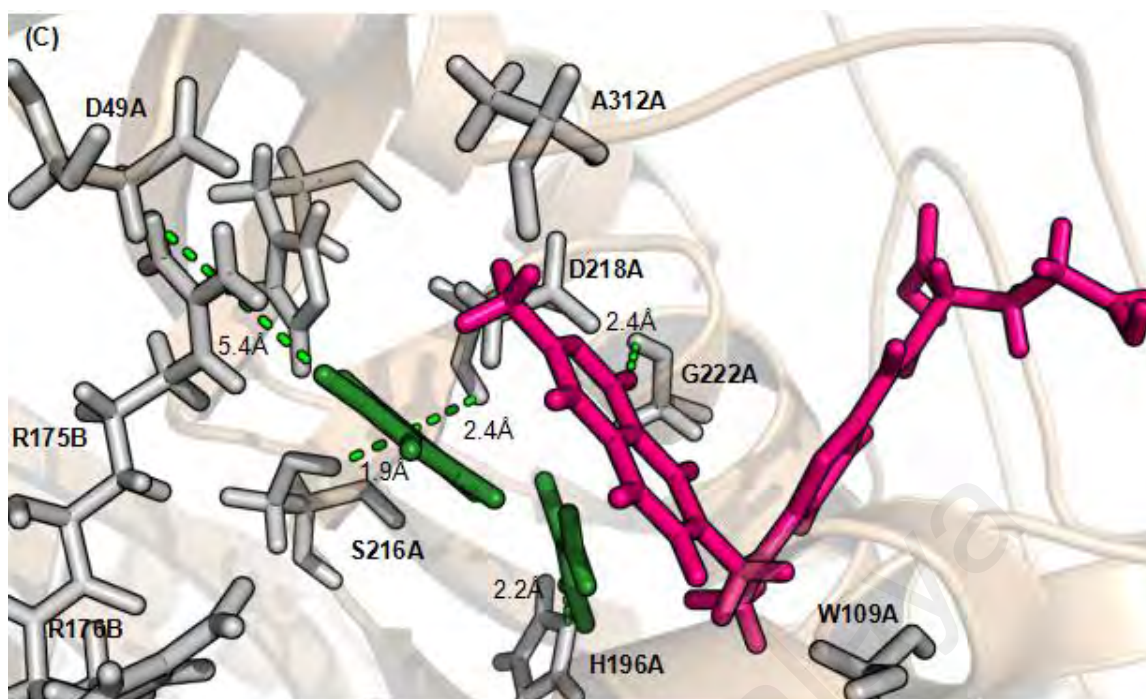


Figure 4.3, continued

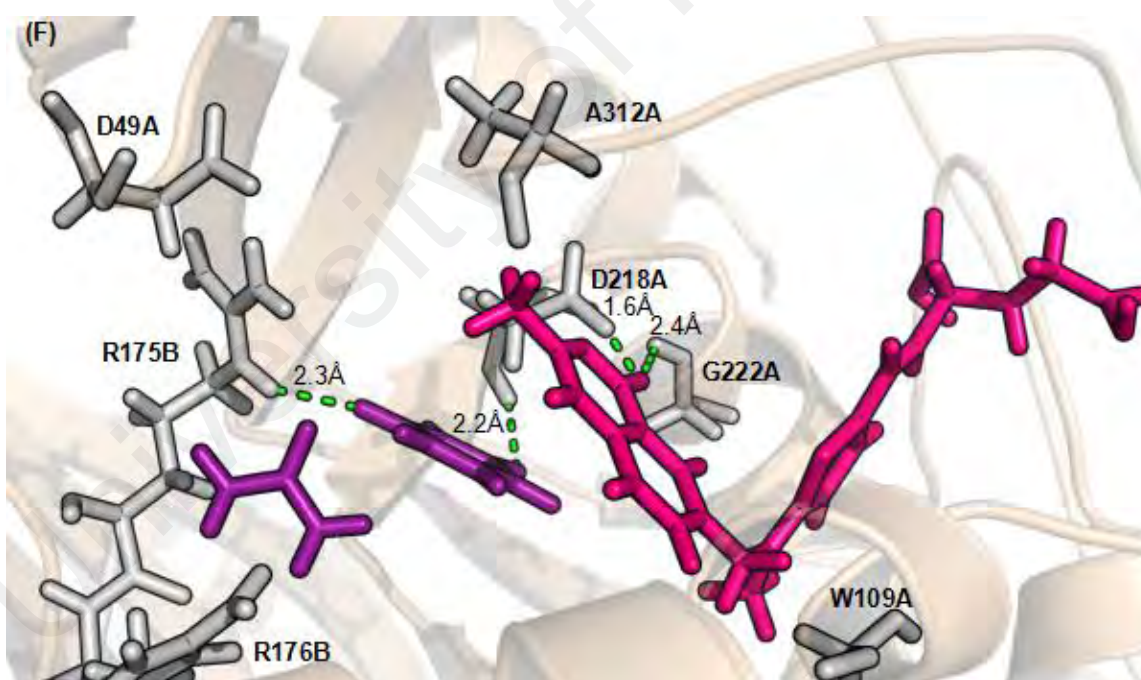
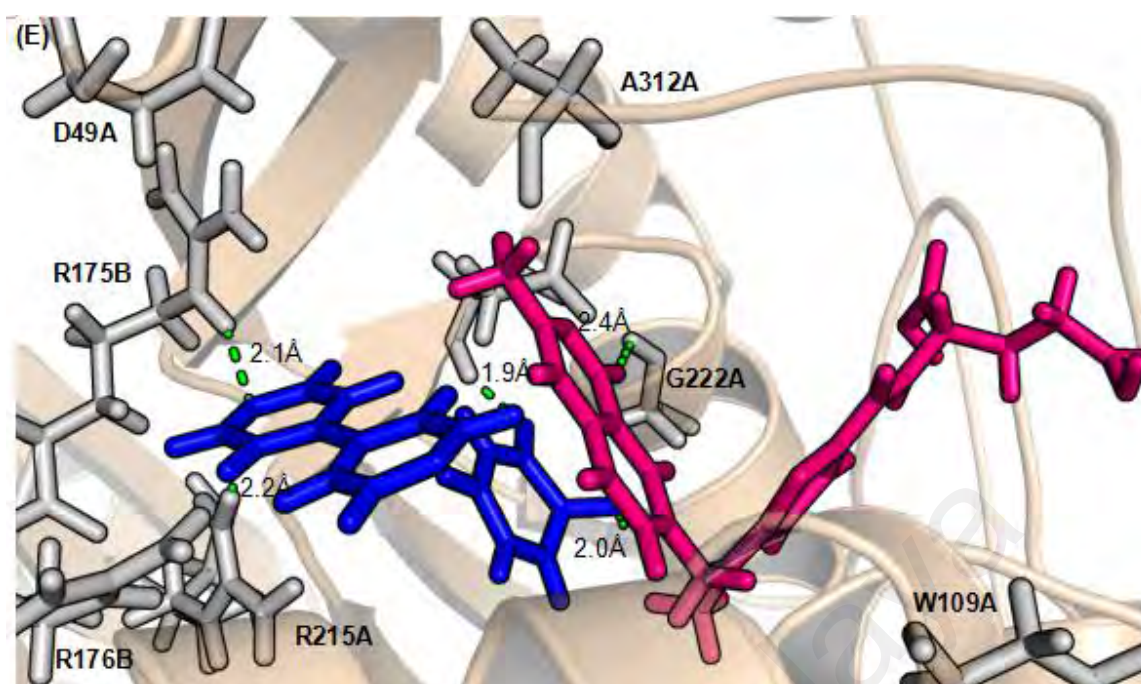
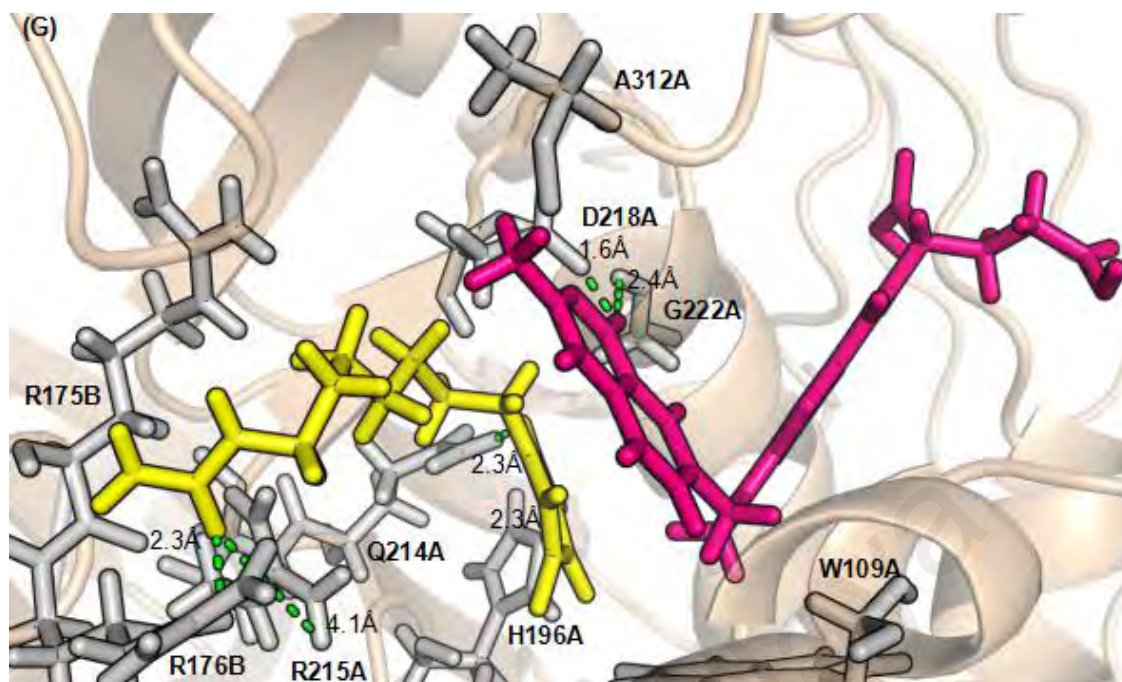


Figure 4.3, continued



**Figure 4.3, continued**

In contrast, there is only one hydrogen bond in a raltitrexed-5FU-22 co-crystal complex. The raltitrexed-5FU-44 co-crystal complex shows hydrogen bonding between 5FU-44 co-crystal with Arg215A, Asp218A, Asn226A, and Arg175B whilst raltitrexed have hydrogen bonding with Gly222A. Further insights into the raltitrexed-UU co-crystal complex, both raltitrexed and UU co-crystal have hydrogen bonding with Asp218A. The modification co-crystal in the presence of raltitrexed (raltitrexed-compound 1 complex) showed better results with several hydrogen bonds with Gln214A, Arg215A, Gly222A, Arg176B, Asp218A, and His196A residues. The majority of the complexes have hydrogen bonds with Arg215A, Arg175B, Arg176B, Asp218A and Gly222A residues indicating that residues play important role in the stability and the strength of complexes.

#### **4.1.2 Stability and Flexibility of Protein-ligand Complexes**

The stability of the docking complexes was assessed by probing the stability via molecular dynamic simulations. Root Mean Square Deviation (RMSD) of all C $\alpha$  atoms

(Figure 4.4) examined the structural properties and dynamic conformational changes of all complexes. The raltitrexed-5FU-U co-crystal complex was stable at the beginning of the simulations, however it showed instability starting from 22 ns trajectory with fluctuation at the range (2.3 Å -4.8 Å). Inspection of individual frames after 26 ns trajectory revealed that 5FU-U co-crystal has been removed from the binding site during long run simulation, thus unable to enhance the binding affinity of raltitrexed with TS (Figure 4.5).

On the other side, the raltitrexed-compound 1 complex was stable with the least fluctuation along the simulations at the range (1.8 Å -3.8 Å). In fact, this complex was more stable compared to the raltitrexed-dUMP complex at longer simulation starting from 35 ns trajectories. Hence, this finding indicates that compound 1 can improve the stability of raltitrexed complex and it was carried forward for the binding energy calculation.

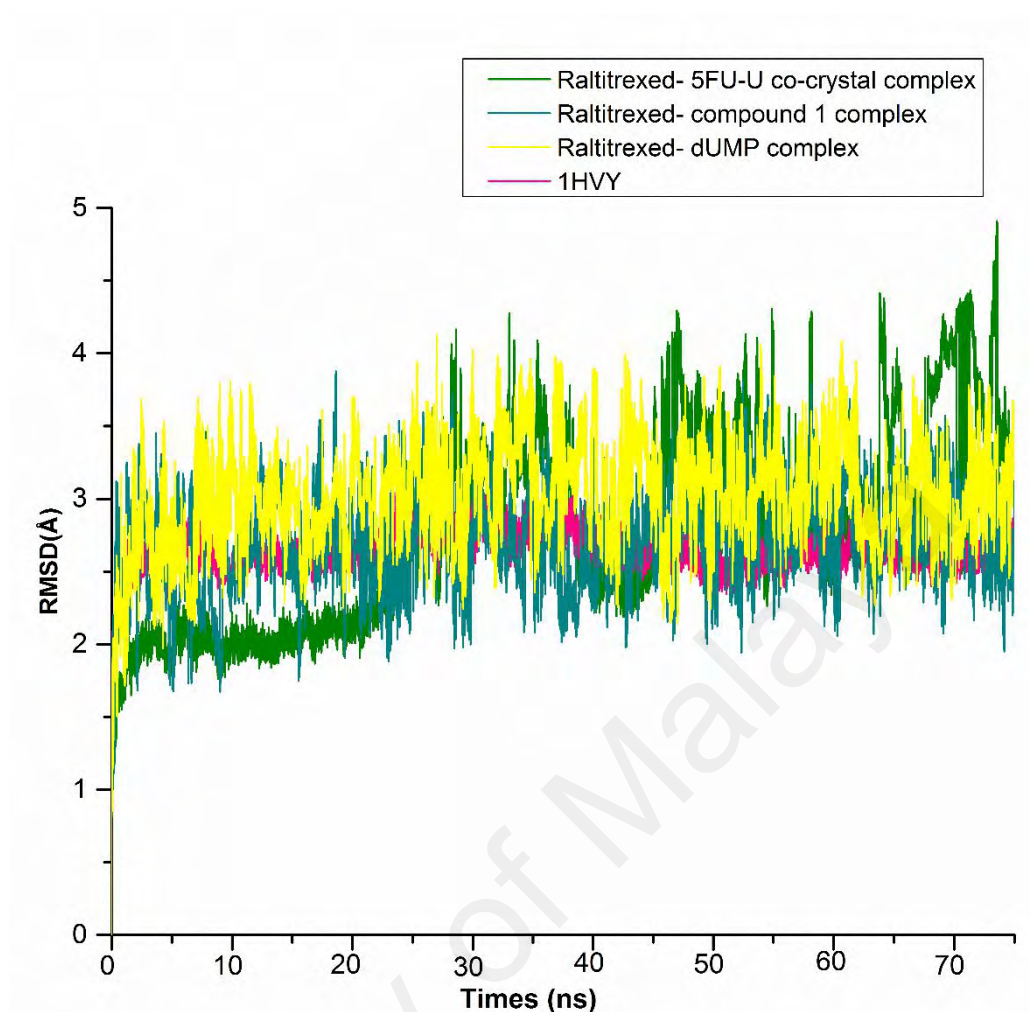


**Figure 4.4:** Molecular dynamic trajectory plot correlating root mean square deviation (Å) of raltitrexed-5FU-U co-crystal complex, raltitrexed-compound 1 complex and raltitrexed-dUMP complex within 75 ns simulation.

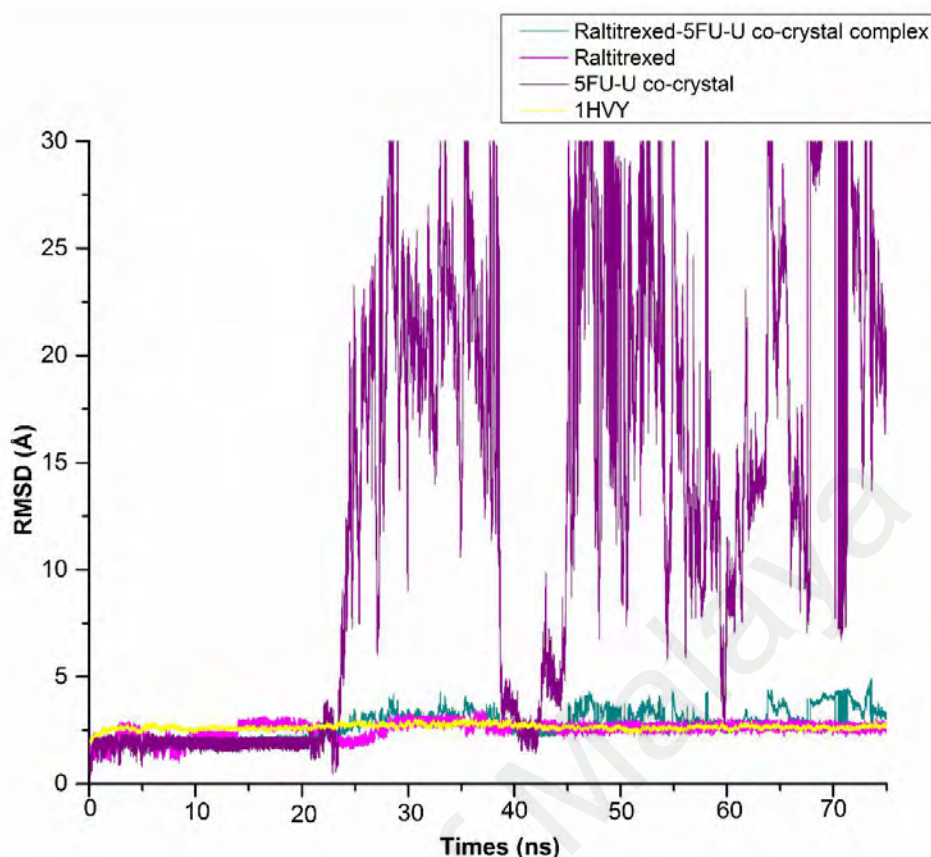


**Figure 4.5: Inspection of individual frame in raltitrexed-5FU-U co-crystal complex along the simulation.**

#### 4.1.3 Binding Free Energy Calculation (MM-PBSA/GBSA)

The relative binding free energy contributions for the protein-ligand complexes based on MM-PBSA/GBSA were extracted from the last 5 ns of simulation for each complex. The results are summarized in Table 4.1. MM-PBSA/GBSA calculations suggested that the van der Waals (vdW) force makes a major contribution to the raltitrexed-dUMP complex binding. In contrast, the contribution of binding energy for raltitrexed-compound 1 complex contributed from the electrostatic interaction (ELE).

The negative values of binding free energy of both complexes in the MM-PBSA/GBSA method demonstrated clearly that these complexes were favorable in water. As expected, the GBSA approach indicates lower binding free energy rather than PBSA approach since there was no metal in this system. GB model is the best model to

evaluate the binding affinities of inhibitor and binding affinities of systems without metals (Hou et al., 2011). The compound 1 decreases the total binding free energy of raltitrexed complex as calculated by GBSA from  $-16.57 \pm 15.62$  kcal/mol to  $-45.68 \pm 15.82$  kcal/mol. The high standard deviations caused by long simulation had been done. The effectiveness of standard deviation was reduced, as the length of simulation is increased (Genheden & Ryde, 2009). Thus, this finding revealed that compound 1 enhance the binding affinity of raltitrexed.

**Table 4.1: MM-PBSA/GBSA calculation within last 5 ns MD simulations.**

		Raltitrexed- dUMP complex	Raltitrexed- compound 1 complex
MM	ELE	$-18.76 \pm 19.80$	$-88.25 \pm 30.88$
	VDW	$-23.66 \pm 22.06$	$-64.14 \pm 21.85$
PBSA	PB <sub>SUR</sub>	$-3.75 \pm 3.48$	$-9.17 \pm 3.08$
	PB <sub>CAL</sub>	$29.09 \pm 28.40$	$124.00 \pm 42.30$
	PB <sub>SOL</sub>	$25.34 \pm 25.06$	$114.84 \pm 39.31$
	PB <sub>ELE</sub>	$10.33 \pm 10.01$	$35.75 \pm 13.20$
	PB <sub>TOT</sub>	$-17.07 \pm 16.24$	$-37.56 \pm 14.04$
GBSA	GB <sub>SUR</sub>	$-2.15 \pm 2.00$	$-6.12 \pm 2.06$
	GB <sub>CAL</sub>	$27.99 \pm 27.52$	$112.84 \pm 38.64$
	GB <sub>SOL</sub>	$25.84 \pm 25.59$	$106.72 \pm 36.65$
	GB <sub>ELE</sub>	$9.23 \pm 8.83$	$24.59 \pm 8.97$
	GB <sub>TOT</sub>	$-16.57 \pm 15.62$	$-45.68 \pm 15.82$

Note: ELE accounts for the electrostatic interactions. VDW denotes for Van der Waals interaction between the fragments, PB<sub>SUR</sub> denotes for the non-polar contribution to solvation, PB<sub>CAL</sub> is the polar contribution of solvation, PB<sub>SOL</sub> is the total of PB<sub>SUR</sub> + PB<sub>CAL</sub>, PB<sub>ELE</sub> account for the PB<sub>CAL</sub> + ELE addition, and PB<sub>TOT</sub> represents for the total binding free energy calculated by the MM-PBSA method.

#### 4.1.4 Key Interactions Residues Involving in the Binding Sites of the Complexes

In order to identify the key residues involved in the binding of the complexes, per-residue free energy decomposition had been performed. Details of the key residues that contribute to the complex binding in the nucleotide and folate binding sites have been interpreted in Figure 4.6 and 4.7. Concerning nucleophilic catalysis is a chemical reaction that responsive to TS catalysis, catalytic Cys195A has played a pivotal role in nucleotide binding site (Santi, 1968). The data revealed that raltitrexed-compound 1 complex has better interactions with Cys195A residue rather than dUMP-raltitrexed complex.

Due to the analysis of interaction residues in a raltitrexed-compound 1 complex, the strong interaction with His196A is mainly contributed from the electrostatic interaction. In fact, direct interaction between the His196 imidazole and an O4 atom has been observed in the complexes of mammalian species (Phan et al., 2001). Moreover, the binding of raltitrexed-compound 1 complex was enhanced by the interactions with Arg50A, Leu192A, and Asn226A residues whilst Gly217A residue has been observed to interact with both complexes. In the folate binding site, Phe80A, Ile108A, Trp109A, Asp218A, Phe225A, Tyr258, Met311A and Ala312A were key residues that decreased the binding energy of the complexes. The calculation also suggested that raltitrexed-compound 1 has better interaction with the key residues compared to the raltitrexed-dUMP complex. Overall, the majority of interactions for both complexes in the folate-binding site mainly comes from the electrostatic interaction rather than van der Waals forces.

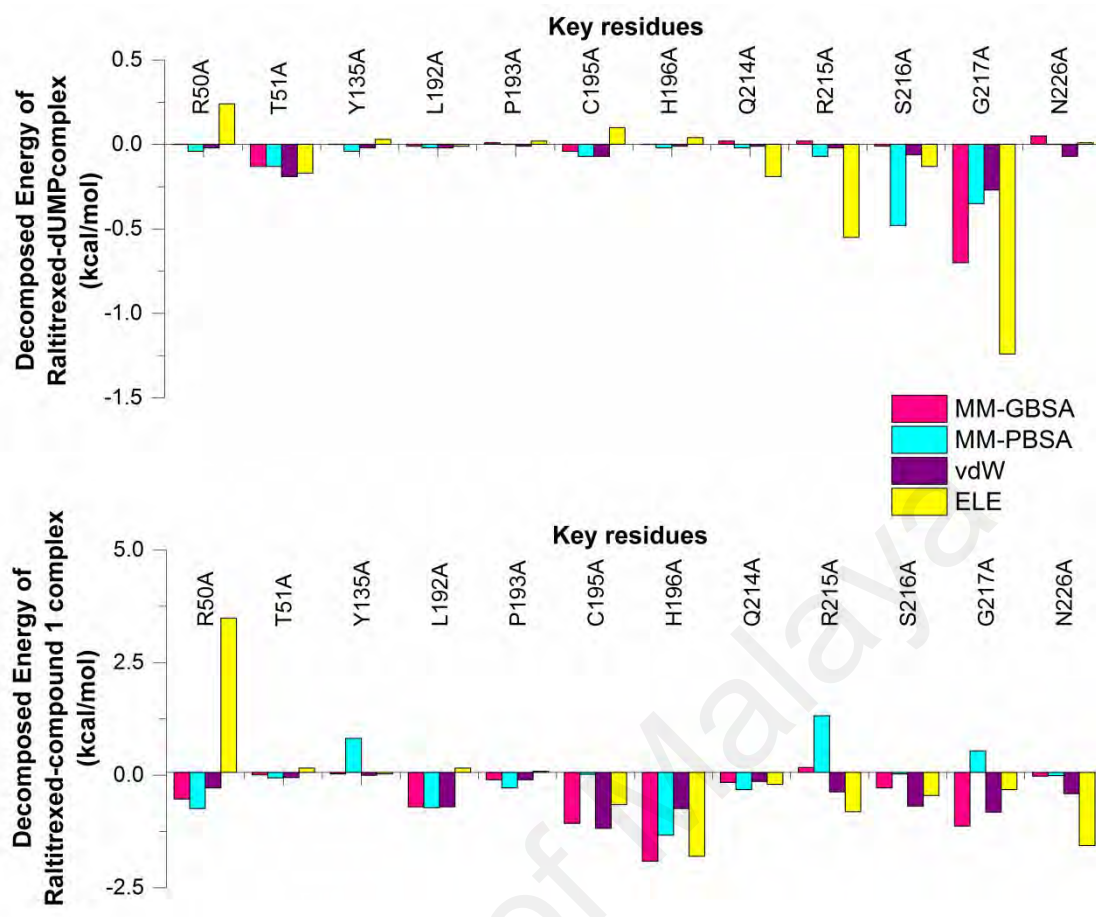


**Figure 4.6: Key interaction residues within 4 (Å) in the nucleotide binding site that contribute to the binding strength of complexes.**

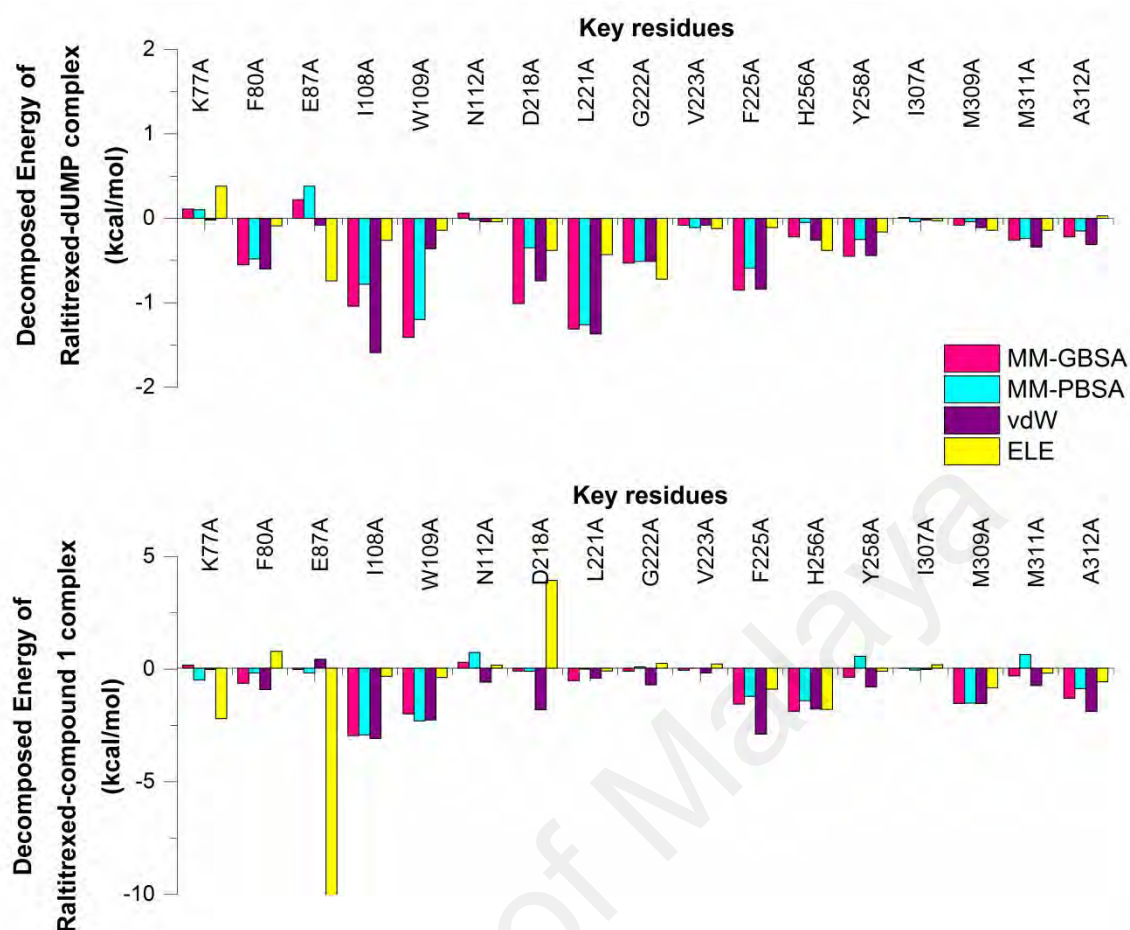


**Figure 4.7: Key interaction residues within 4 (Å) in the folate binding site that contribute to the binding strength of complexes.**

Molecular dynamic simulations can explicitly analyze hydrogen bond properties such as donor-acceptor position and hydrogen bond occupancies. A hydrogen bond is one of the factors that influence the affinity between protein and ligand (Wikinson et al., 1984). The percentage detail occupations of hydrogen bonds in both potential binding sites within last 5 ns are represented in Figure 4.8.

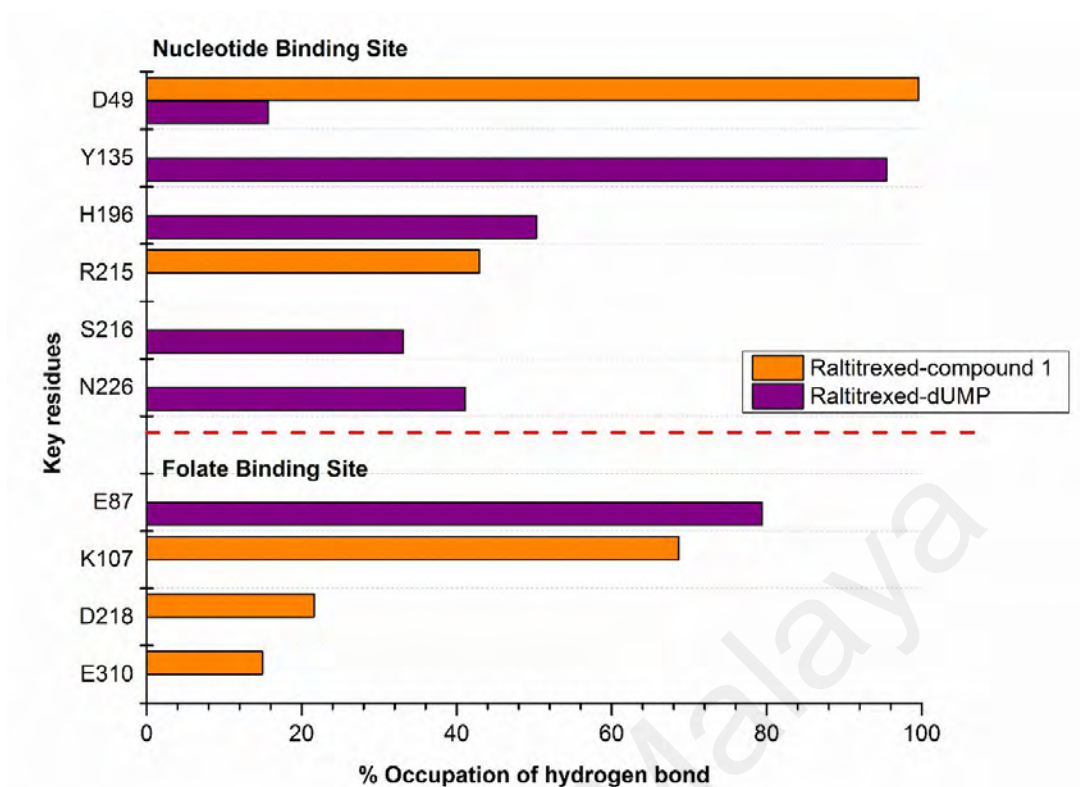


**Figure 4.8: The percentage of hydrogen bonds occupied per residue within last 5 ns.**

From the result, the raltitrexed-compound 1 complex exhibited higher percentage occupation of intermolecular H-bond formation rather than raltitrexed-dUMP complex for both nucleotide and folate binding sites. For the nucleotide binding site, Asp49A and Arg215A residues play a significant role in a raltitrexed-dUMP complex with 99.60% and 42.92% of hydrogen bonds occupied between dUMP(OH)---(O)Asp24A and Arg215A(NH)---(O)dUMP. In contrast, strong hydrogen bonds formation of raltitrexed-compound 1 complex have been observed between Tyr135A(OH)---(O)compound 1 with 95.44% whilst moderate hydrogen bonds formed between compound 1(NH)---(N)His196A, Asn226A(NH)---(O)compound 1 and Ser191A(OH)---(O)compound 1 with 50.32%, 41.12% and 33.12% of occupation, respectively.

Meanwhile, in the folate-binding site, there were moderate percentage of hydrogen bonds occupied between raltitrexed with Lys107A, Asp218A, and Glu310A with

68.96%, 21.60%, and 14.92% in raltitrexed-dUMP complex. Raltitrexed-compound 1 complex exposed contradict result with tight intermolecular hydrogen bonds formed complex between raltitrexed(OH)---(O)Glu87A with 79.44% of hydrogen bonds occupied. The majority of intermolecular hydrogen bonds formed were considered as the satisfied hydrogen bonds since hydrogen-acceptor distance  $\leq 2.5\text{\AA}$  and an angle close to  $180^\circ$ .

Due to the analysis by PLIP, the green dotted lines represent the predicted hydrogen bond of the complexes, blue dotted lines remark hydrophobic interaction, red dotted lines highlight the perpendicular  $\pi$ -stacking interaction and orange dotted lines shows the salt bridge formation. According to the non-covalent interaction analysis for both complexes at 75 ns trajectory (Figure 4.9), there is a conformational change of receptor upon ligand binding for raltitrexed-compound 1 complex since compound 1 is larger than dUMP.

For the raltitrexed-dUMP complex, dUMP shows hydrogen bonding with Asp49A, and Arg175B at 75ns trajectory. Further, there is salt bridge formation caused by closed interaction between Arg215A and Arg176B. Meanwhile, raltitrexed exhibited hydrogen bonds formation with Gly105A, Lys107A, Asp218A, and Ala312A residues. In addition, there are hydrophobic interactions between raltitrexed with Phe80A, Ile108A, Asp218A, and Leu196A whilst the favorable perpendicular  $\pi$ -cation interaction with Phe225A formed caused by the interaction of cation with a negative charge when the cation is nearby the face of  $\pi$ -system. For the raltitrexed-compound 1 complex, compound 1 has engaged with hydrogen bonds at Asp49A, Tyr135A, and Asn226A residues at 75 ns trajectory. Besides, the hydrophobic interaction between compound 1 and Asp218A residue enhance the interaction of the complex. On the other hand, raltitrexed displays

hydrogen bonds with Glu87A and hydrophobic interactions with Trp109A, Tyr258A, and Ala287A residues.

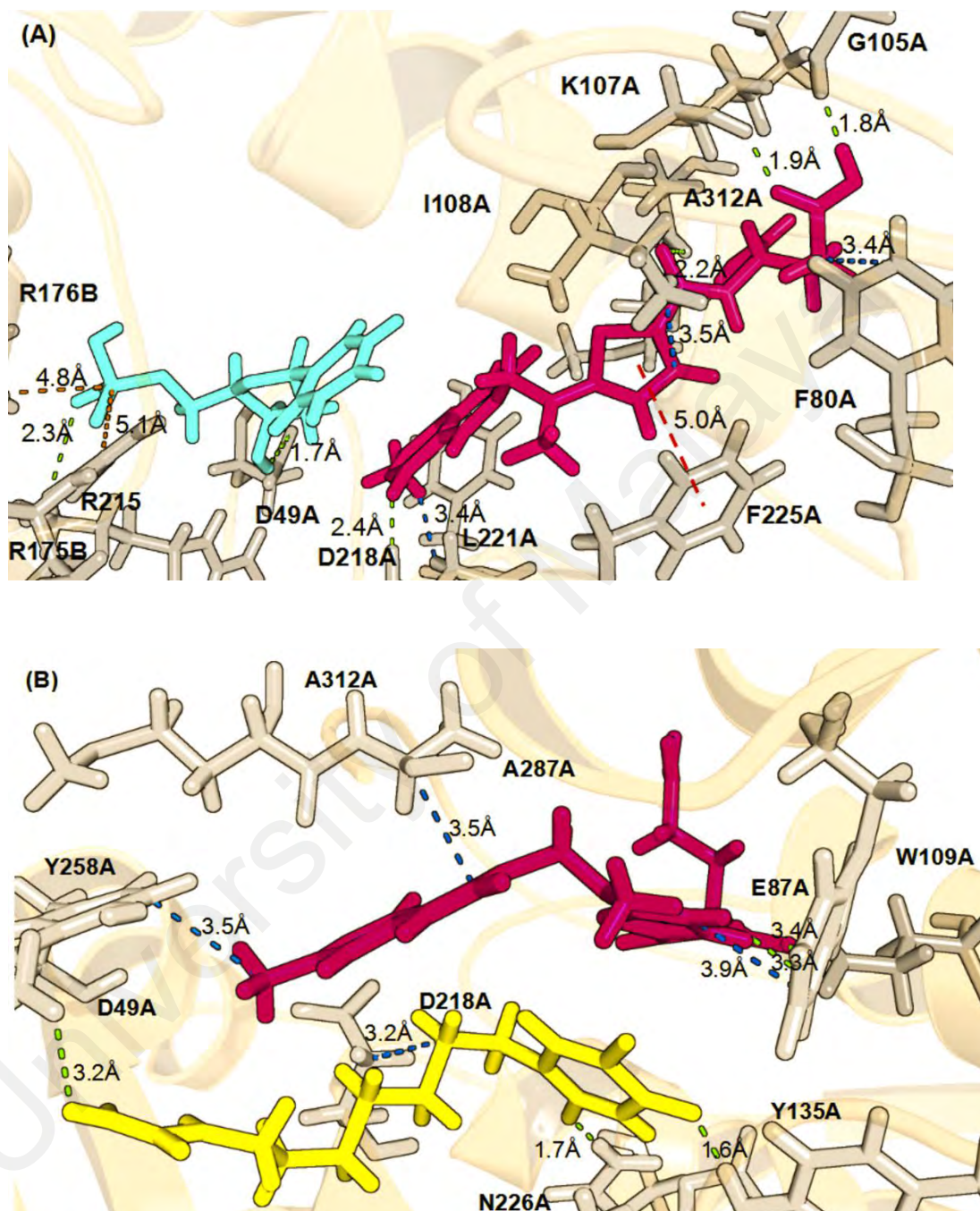


**Figure 4.9:** The non-covalent interaction for (A)raltitrexed(pink)-dUMP(light blue) complex and (B)raltitrexed-compound 1(yellow) complex at 75 ns trajectory.

## 4.2 Drug-likeness Analysis

### 4.2.1 Physicochemical Properties Prediction based on Lipinski's Rule of Five (RO5)

The drug-likeness of raltitrexed and compound 1 were predicted through their physicochemical analysis based on the Lipinski's rule of five (RO5). RO5 predicted to have absorption or permeability problem if the compound has calculated  $\log P > 5$ , molecular weight (MW)  $> 500$ , hydrogen bond donor  $> 5$  or hydrogen bond acceptor  $> 10$ . Log P refer to the octanol-water coefficient to measure the lipophilicity of drug meanwhile any oxygen and nitrogen atom are considered as a hydrogen bond acceptor whilst N-H or O-H are considered as a hydrogen bond donor (Lipinski et al., 1997). Briefly, both ligands are predicted to overcome the absorption problem since they have  $\log P < 1$ , molecular weight  $< 500$ , hydrogen bond acceptor  $< 10$  and hydrogen bond donor  $< 5$ . Thus, this combination of treatment has high possibility to overcome the drug delivery barrier. All the data are summarized in Table 4.2.

**Table 4.2: Physicochemical properties prediction of ligands.**

Ligands	Predicted physicochemical properties				
	Log P	Hydrogen Acceptor Count	Hydrogen Donor Count	Polar Surface Area ( $\text{\AA}^2$ )	Molecular Weight ( $\text{g mol}^{-1}$ )
Raltitrexed	0.89	8	3	176.64	458.49
Compound 1	-0.21	3	3	104.53	286.30

### 4.2.2 ADMET Prediction for 2D QSAR

ADMET is widely used as a first step to predict pharmacokinetics properties and prevent wasting time on lead candidates that would be toxic or not permeable to cross membranes. The ADMET prediction has been carried out to investigate the pharmacokinetic of raltitrexed, 5-FU and compound 1. The result was analyzed and

reported in Table 4.3. The bi-plot (Figure 4.10) shows the two analogous 95% and 99% confidence ellipse corresponding to the HIA and BBB models.

Polar surface area (PSA) was demonstrated to have an inverse relationship with percent human intestinal absorption and cell wall permeability. Thus, a model with descriptors AlogP98 and PSA\_2D with bi-plot consist of 95% and 99% confidence ellipse was considered as an accurate prediction for the cell permeability of compounds. The 95% confidence ellipse shows the region of chemical space that we can expect to find well-absorbed compound whilst 99% confidence ellipse represents the region of chemical space with compounds having excellent absorption via cell membrane. The result showed that 5-FU and compound 1 were predicted to have optimum cell permeability with PSA <140Å<sup>2</sup> and AlogP98 <5 (Egan et al., 2000).

**Table 4.3: ADMET prediction of ligands.**

Ligand	Raltitrexed	5-FU	Compound 1
ADMET AlogP98	2.527	-0.908	0.291
ADMET unknown AlogP98	0	0	0
ADMET PSA_2D	153.033	60.222	107.415
ADMET BBB level	4	3	3
ADMET absorption level	3	1	0
ADMET solubility	-3.9	-0.081	-1.261
ADMET solubility level	3	4	4
ADMET hepatotoxicity	1	1	1
ADMET hepatotoxicity probability	0.754	0.834	0.582
ADMET CYP2D6	0	0	0
ADMET CYP2D6 probability	0.297	0.019	0.346
ADMET PPB level	0	0	0

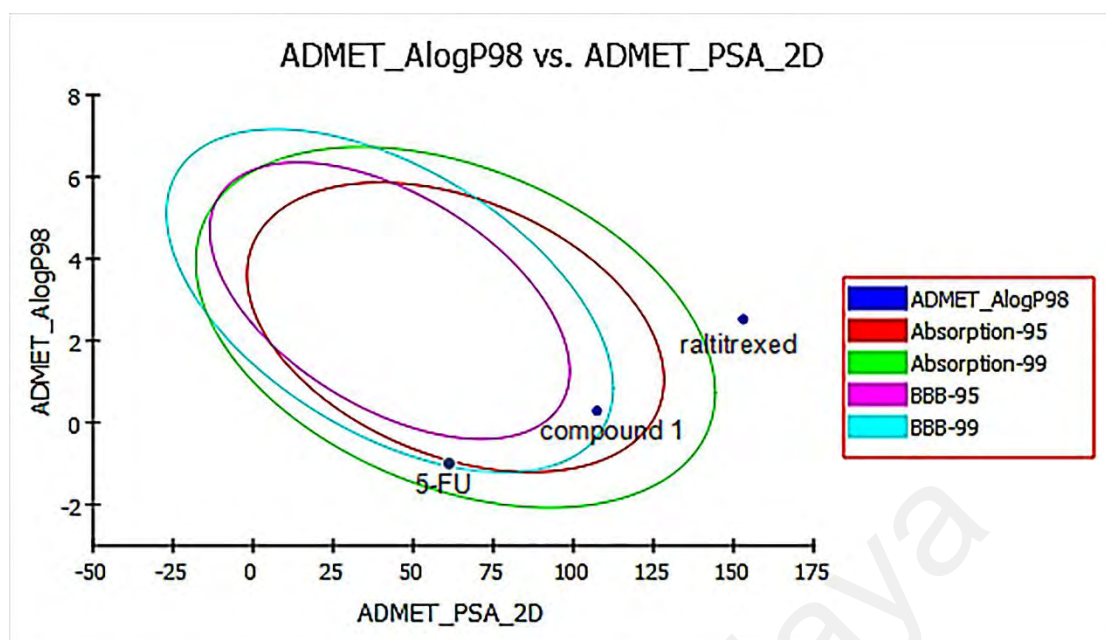


**Figure 4.10: 2D polar surface area (PSA<sub>2D</sub>) for each compound is plotted against their corresponding calculated atom-type partition coefficient (ALogP98) based on absorption model the 95% and 99% confidence limit ellipses corresponding to the Blood Brain Barrier(BBB) and Intestinal Absorption Model (Egan et al., 2000).**

Since all ligands have been predicted to have low value for BBB penetration levels, they may not be able to penetrate into the blood-brain barrier and reduce the chances of CNS side effects. In fact, compound 1 has improved the ability to absorb well through human intestinal with lower ADMET absorption level rather than 5-FU and raltitrexed. In term of solubility, they are predicted to have high dissolution rate since they have optimal aqueous solubility level. Further analysis with hepatotoxicity, compound 1 was found to have less toxicity compared to raltitrexed and 5-FU with lower hepatotoxicity probability.

In addition, all ligands were predicted to have low CYP2D probability. Therefore, the liver dysfunction side effect is not expected upon administration of these compounds and indicates that they are well-metabolized (Venkataramana et al., 2011). However, ADMET plasma protein binding (PPB) property prediction denotes that they have

binding <90% since the PPB level is 0. Overall, compound 1 shows the potential as a drug candidate with the best pharmacokinetic properties.

University of Malaya

## CHAPTER 5: CONCLUSION

Pharmaceutical co-crystals have emerged as a new alternative to overcome the intrinsic barrier of drug delivery. However, computational studies revealed that 5FU-U co-crystal is unstable along the molecular dynamic simulation; hence, it cannot enhance the binding affinity of raltitrexed in thymidylate synthase inhibition. The combination of raltitrexed with other anti-cancer agents promises better result than monotherapy. The computational approach reveals that the modified based co-crystal, compound 1 has improved the stability of co-crystal, thus enhancing the binding affinity of raltitrexed (-45.68 kcal/mol) rather to raltitrexed alone (-16.57 kcal/mol). Decomposition energy per residue suggested that Arg50A, Leu192A, Cys195A, His196A, Asn226 and Gly217A are pivotal residues that play the main role in nucleotide binding site. The binding free energy in folate binding site majority is from Phe80A, Ile108A, Trp109A, Asp218A, Phe225A, Tyr258A, Met311A and Ala312A residues. The result from ADMET indicates that compound 1 has good pharmacokinetic properties with optimum permeability and less toxicity than 5-FU. Hence, compound 1 can be further explored and developed as one of the potential anti-cancer drugs.

## REFERENCES

- Aakeroy, C. B. & Salmon, D. J. (2005). Building co-crystals with molecular sense and supramolecular sensibility. *CrystEngComm*, 7, 439-448.
- Aakeroy, C.B., Fasulo, M., Scultheiss, N., Desper, J., & Moore, C. (2007). Structural competition between hydrogen bonds and halogen bonds. *Journal of American Chemical Society*, 129, 13772-13773.
- Aakeroy, C. B., Forbes, S., & Desper, J. (2009). Using cocrystals to systematically modulate aqueous solubility and melting behavior of an anticancer drugs. *Journal of American Chemical Society*, 131, 17048-17049.
- ACS (2015). *American Cancer Society*. Retrieved from <http://www.cancer.org/cancer/colonandrectumcancer/detailedguide/colorectal-cancer-what-is-colorectal-cancer>.
- Aitipamula, S., Banerjee, R., Bansal, A. K., Biradha, K., Cheney, M. L., Choudhury, A. R., ... Zaworotko, M. J. (2012). Erratum: Polymorphs, salts and cocrystals: What's in a name? *Crystal Growth and Design*, 12(8), 4290–4291.
- Almarsson, O. & Zawotko, M. J. (2004). Crystal engineering of the composition of pharmaceutical phases. Do pharmaceutical co-crystals represent a new path to improved medicines? *Chemical Communication*, 17, 1889 -1896.
- Amin, K., Dannenfelser, R. –M., Zielinski, J. and Wang, B. (2004). Lyophilization of polyethylene glycol mixtures. *Journal of Pharmaceutical Sciences*, 93, 2244-2249.
- Appelt, K., Bacquet, R. J., Bartlett, C. A., Booth, C. L. J., Freer, S. T., Fuhry, M. A. M., ... Howl (1991). Design of enzyme inhibitors using iterative protein crystallographic analysis. *Journal of Medicinal Chemistry*, 34(7), 1925-1934.
- Archontis, G., Simonson, T., & Karplus, M. (2001). Binding free energies and free energy components from molecular dynamics and Poisson-Boltzmann calculations. Application to amino acid recognition by aspartyl-tRNA synthetase1. *Journal of Molecular Biology*, 306(2), 307–327.
- Bauer, J., Spanton, S., Henry, R., Quick, J., Dziki, W., Porter, W., & Morris, J. (2001). Ritonavir: An extraordinary example of conformational polymorphism. *Pharmaceutical Research*, 18, 859-866.
- Bayly, C. I., Cieplak, P., Cornell, W., & Kollman, P. A. (1993). A well-behaved electrostatic potential based method using charge restraints for deriving atomic charges: The RESP model. *The Journal of Physical Chemistry*, 97(40), 10269–10280.
- Becke, A. D. (1993). Density-functional thermochemistry. III. The role of exact exchange. *The Journal of Chemical Physics*, 98(7), 5648-5642.

- Becker, O. M., MacKerell, A. D., Roux, B., & Watanabe, M (2001). *Computational Biochemistry & Biophysic*. USA: CRC Press.
- Berger, S. H., Berger, F. G., & Lebioda, L. (2004). Effects of ligand binding and conformational switching on intracellular stability of human thymidylate synthase. *Biochimica et Biophysica Acta - Proteins and Proteomics*, 1696(1), 15–22.
- Bertino, J. R., & Banerjee, D. (2004). Thymidylate synthase as an oncogene? *Cancer Cell*, 5(4), 301–302.
- Bissantz, C., Kuhn, B., & Stahl, M. (2010). A medicinal chemist's guide to molecular interactions. *Journal of Medicinal Chemistry*, 53(14), 5061-5084.
- Blagden, N., de Matas, M., Gavan, P.T., & York, P. (2007). Crystal engineering of active pharmaceutical ingredients to improve solubility and dissolution rates. *Advanced Drug Delivery Review*, 59, 617-630.
- Bleicher, K. H., Böhm, H. J., Müller, K., & Alanine, A. I. (2003). Hit and lead generation: Beyond high-throughput screening. *Nature Reviews Drug Discovery*, 2(5), 369-378.
- Braga, D., Grepioni, F., Maini, L., Properi, S., Gobetto, R., & Chierotti, M. R. (2010). From unexpected reactions to a new family of ionic co-crystals: The case of barbituric acid with alkali bromides and caesium iodide. *Chemical Communications*, 46(41), 7715-7717.
- Bronson, J., Black, A., Dhar, T. G. M., Ellsworth, B. A. & Merritt, J. R. (2013). To market, to market-2012. *Annual Report in Medicinal Chemistry*, 48, 471-546.
- Brooks, B. R., Brooks, C. L., Mackerell, A. D. J., Nilsson, L., Petrella, R. J., Roux, B., ... Karplus, M. (2009). CHARMM: The biomolecular simulation program. *Journal of Computational Chemistry*, 30(10), 1545–1614.
- Brough, P. A., Barril, X., Borgognoni, J., Chene, P., Davies, N. G., Davis, B., ... Fromont, C. (2009). Combining hit identification strategies: Fragment-based and in silico approaches to orally active 2-aminothieno [2, 3-d] pyrimidine inhibitors of the Hsp90 molecular chaperone. *Journal of Medicinal Chemistry*, 52(15), 4794-4809.
- Burgoyne, N. J., & Jackson, R. M. (2006). Predicting protein interaction sites: Binding hot-spots in protein–protein and protein–ligand interfaces. *Bioinformatics*, 22(11), 1335-1342.
- Buroker, T. R., O'Connell, M. J., Wieand, H. S., Krook, J. E., Gerstner, J. B., Mailliard, J. A., ... Gesme, D. H. (1994). Randomized comparison of two schedules of fluorouracil and leucovorin in the treatment of advanced colorectal cancer. *Journal of Clinical Oncology*, 12(1), 14-20.
- Byrn, S. R., Pfeiffer, R. R., & Stowell, J. G. (1999). *Solid State Chemistry of Drugs* (2nd Ed). West Lafayette, Indiana: SSCI Inc.

- Caradonna, S. J., & Cheng, Y-C (1980). The role of deoxyuridine triphosphate nucleotidohydrolase, uracil-DNA glycosylase, and DNA polymerase  $\alpha$  in the metabolism of FUdR in human tumor cells. *Molecular Pharmacology*, 18, 513-520.
- Carreras, C. W., & Santi, D. V. (1995). The catalytic mechanism and structure of thymidylate synthase. *Annual Review of Biochemistry*, 64, 721–762.
- Case, D. A., Darden, T. A., Cheatham, TEIII., Simmerling, C. L., Wang, J., Duke, R. E., Luo, R., Walker, R. C., Zhang, W., Merz, K.M., Roberts, B., Hayik, S., Roitberg, A., Seabra, G., Swails, J., Goetz, A.W., Kolossváry, I., Wong, K.F., Paesani, F., Vanicek, J., Wolf, R.M., Liu, J., Wu, X., Brozell, S.R., Steinbrecher, T., Gohlke, H., Cai, Q., Ye, X., Wang, J., Hsieh, M. J., Cui, G., Roe, D. R., Mathews, D. H., Seetin, M. G., Salomon-Ferrer, R., Sagui, C., Babin, V., Luchko, T., Gusarov, S., Kovalenko, A., & Kollman, P.A. (2012). *AMBER 12*. University of California, San Francisco.
- Cheng, A., & Dixon, S. L. (2003). In silico models for the prediction of dose-dependent human hepatotoxicity. *Journal of Computer-Aided Molecular Design*, 17(12), 811–823.
- Cheng, N., Hubert, M., Saville, D., Rades, T., & Aaltonen, J. (2009). Formation kinetics and stability of carbamazepine-nicotinamide cocrystals prepared by mechanical activation. *Crystal Growth & Design*, 9, 2377-2386.
- Cheung, D. Y., Kim, T. H., Kim, C. W., Kim, J. I., Cho, S. H., Park, S. H., Han, J. Y. & Kim, J. K. (2008). The anatomical distribution of colorectal cancer in Korea: Evaluation of the incidence of proximal and distal lesions and synchronous adenomas. *Internal Medicine Journal*, 47, 1647-1654.
- Cho, E., Cho, W., Cha, K.H., Park, J., Kim, M.-S., Park, H. J., & Hwang, S.-J. (2010). Enhanced dissolution of magesrol acetate microcrystals prepared by antisolvent precipitation process using hydrophilic additives. *International Journal of Pharmaceutics*, 396, 91-98.
- Coates, G. W., Dunn, A. R., Henling, L. M., Ziller, J. W., Lobkovsky, E. B., & Grubbs, R. H. (1998). Catalytic for the living insertion polymerization with chiral catalysts: New opportunities for stereocontrol using polymer exchange mechanisms. *Journal of the American Chemical Society*, 120(15), 3641-3659.
- Dai, Y., Wang, Q., Zhang, X., Jia, S., Zheng, H., Feng, D., & Yu, P. (2010). Molecular docking and QSAR study on steroidal compounds as aromatase inhibitors. *European Journal of Medicinal Chemistry*, 45(12), 5612–5620.
- Danenberg, P. V., Leichman, L., Lenz, H. J., Leichman, C. G., & Danenberg, K. D. (1995). Thymidylate synthase gene and protein expression correlate and are associated with response to 5-fluorouracil in human colorectal and gastric tumors. *Cancer Research*, 55(7), 1407–1412.
- Danenberg, P.V. (1977). Thymidylate synthase – a target enzyme in cancer chemotherapy. *Biochim Biophys Acta* , 473(2), 1925-1934.

- Davies, M. M., Johnston, P. G., Kaur, S., & Allen-mersh, T. G. (1999). Colorectal liver metastasis thymidylate synthase staining correlates with response to hepatic arterial floxuridine colorectal liver metastasis thymidylate synthase staining correlates with response to hepatic arterial floxuridine. *Clinical Cancer Research*, 5, 325–328.
- Desiraju, G. R. (1995). Supramolecular synthons in crystal engineering-a new organic synthesis. *Angewandte Chemie International Edition*, 34, 2311-2327.
- Dixon, S. L., & Merz, K. M. (2001). One-dimensional molecular representations and similarity calculations: Methodology and validation. *Journal of Medicinal Chemistry*, 44(23), 3795-3809.
- Dolinsky, T. J., Nielsen, J. E., McCammon, J. A., & Baker, N. A. (2004). PDB2PQR: an automated pipeline for the setup of Poisson-Boltzmann electrostatics calculations. *Nucleic Acids Research*, 32, W665-7.
- Douillard, J. Y., Siena, S., Cassidy, J., Tabernero, J., Burkes, R., Barugel, M., ... Rivera, F. (2010). Randomized, phase III trial of panitumumab with infusional fluorouracil, leucovorin, and oxaliplatin (FOLFOX4) versus FOLFOX4 alone as first-line treatment in patients with previously untreated metastatic colorectal cancer: the PRIME study. *Journal of Clinical Oncology*, 28(31), 4697-4705.
- Duggirala, N. K., Perry, M. L., Almarsson, Ö., & Zaworotko, M. J. (2016). Pharmaceutical cocrystals: Along the path to improved medicines. *Chemical Communication*, 52: 640–655.
- Dunn, M. F. (2001). *Protein–Ligand Interactions: General Description*. USA: John Wiley & Sons, Ltd.
- Dupradeau, F. -Y., Pigache, A., Zaffran, T., Savineau, C., Lelong, R., Grivel, N., ... Cieplak, P. (2010). The R.E.D. Tools: Advances in RESP and ESP charge derivation and force field library building. *Physical Chemistry Chemical Physics*, 12(28), 7821–7839.
- Egan, W. J., & Lauri, G. (2002). Prediction of intestinal permeability. *Advanced Drug Delivery Reviews*, 54(3), 273–289.
- Essmann, U., Perera, L., Berkowitz, M. L., Darden, T., Lee, H., & Pedersen, L. (1995). A smooth particle meshes Ewald potential. *Journal of Chemical Physics*, 103, 8577–8592.
- Etter, M. C., & Frankenbach, G. M. (1989). Hydrogen bond directed cocrystallization as a tool for designing acentric organic solid. *Chemistry of Materials*, 1, 10-12.
- FDA (2014). FDA approves Farxiga to treat type 2 diabetes. *Food and Drug Administration*. Retrieved from <http://www.fda.gov/NewsEvents/Newsroom/PressAnnouncements/ucm380829.htm>.

- FDA (2011). Guidance for industry: regulatory classification of pharmaceutical cocrystals. *Food and Drug Administration*. Retrieved from <http://www.fda.gov/downloads/Drugs/Guidances/UCM281764.pdf>.
- Ferreira, R. S., Simeonov, A., Jadhav, A., Eidam, O., Mott, B. T., Keiser, M. J., ... Shoichet, B. K. (2010). Complementarity between a docking and a high-throughput screen in discovering new cruzain inhibitors. *Journal of Medicinal Chemistry*, 53(13), 4891–4905.
- Freddolino, P. L., Arkhipov, A. S., Larson, S. B., McPherson, A., & Schulten, K. (2006). Molecular dynamics simulations of the complete satellite tobacco mosaic virus. *Structure*, 14(3), 437–449.
- Frisch, M. J., Trucks, G. W., Schlegel, H. B., Scuseria, G. E., Robb, M. A., Cheeseman, J. R., Scalmani, G., Barone, V., Mennucci, B., Petersson, G. A., Nakatsuji, H., Caricato, M., Li, X., Hratchian, H. P., Izmaylov, A. F., Bloino, J., Zheng, G., Sonnenberg, J. L., Hada, M., Ehara, M., Toyota, K., Fukuda, R., Hasegawa, J., Ishida, M., Nakajima, T., Honda, Y., Kitao, O., Nakai, H., Vreven, T., Montgomery, J. A. Jr., Peralta, J. E., Ogliaro, F., Bearpark, M., Heyd, J. J., Brothers, E., Kudin, K. N., Staroverov, V. N., Kobayashi, R., Normand, J., Raghavachari, K., Rendell, A., Burant, J. C., Iyengar, S. S., Tomasi, J., Cossi, M., Rega, N., Millam, J. M., Klene, M., Knox, J. E., Cross, J. B., Bakken, V., Adamo, C., Jaramillo, J., Gomperts, R., Stratmann, R. E., Yazyev, O., Austin, A. J., Cammi, R., Pomelli, C., Ochterski, J. W., Martin, R. L., Morokuma, K., Zakrzewski, V. G., Voth, G. A., Salvador, P., Dannenberg, J. J., Dapprich, S., Daniels, A. D., Farkas, Ö., Foresman, J. B., Ortiz, J. V., Cioslowski, J. & Fox, D. J. (2009). *Gaussian 09*, Wallingford, USA.
- Gao, E., Liu, Q., & Duan, L. (2006). An anticancer metallobenzylmalonate: Crystal structure and anticancer activity of a palladium complex of 2, 2' -bipyridine and benzylmalonate. *Journal of Coordination Chemistry*, 59, 1295-1300.
- Ge, Y., Wu, J., Xia, Y., Yang, M., Xiao, J., & Yu, J. (2012). Molecular dynamics simulation of the complex PBP-2x with drug cefuroxime to explore the drug resistance mechanism of streptococcus suis R61. *PLoS ONE*, 7(4), 1–10.
- Gleeson, M. P., Hersey, A., Montanari, D., & Overington, J. (2011). Probing the links between in vitro potency, ADMET and physicochemical parameters. *Nature Reviews Drug Discovery*, 10(3), 197-208.
- Gohlke, H., Kiel, C., & Case, D. A. (2003). Insights into protein–protein binding by binding free energy calculation and free energy decomposition for the Ras–Raf and Ras–RalGDS complexes. *Journal of Molecular Biology*, 330(4), 891–913.
- Gorlick, R., Metzger, R., Danenberg, K. D., Salonga, D., Miles, J. S., Longo, G. S., Fu, J., Banerjee, D., Klimstra, D., ... Jhanwar, S. (1998). Levels of thymidylate synthase gene expression are observed in pulmonary compared with hepatic metastases of colorectal adenocarcinoma. *Journal of Clinical Oncology*, 16, 1465–1469.

- Götz, A. W., Williamson, M. J., Xu, D., Poole, D., Grand, S. L., & Walker, R. C. (2012). Routine microsecond molecular dynamics simulations with AMBER - Part I: Generalized Born. *Journal of Chemical Theory and Computation*, 8, 1542–1555.
- Grand, S. L., Götz, A.W., & Walker, R. C. (2013). SPFP: Speed without compromise-a mixed precision model for GPU accelerated molecular dynamics simulations. *Computer Physics Communications*, 184, 374–380.
- Groden, J., Thilvers, A., Samowitz, W., Carison, M., & Gelbert, L. (1991). Identification and characterization of the familial adenomatous polyposis coli gene. *Cell*, 66, 589-600.
- Hackbarth, C. J, Chen, D. Z., & Lewis, J. G. (2002). N-alkyl urea hydrox-amic acids as a new class of peptide deformylase inhibitors with antibacterial activity. *Antimicrobial Agents Chemotherapy*, 46, 2752-2764.
- Hardy, L. W., Finer-Moore, J. S, Montfort, W. R, Jones, M. O., Santi, D. V., & Stroud, R. M. (1987). Atomic structure of thymidylate synthase: Target for rational drug design. *Science*, 235(4787), 448-455.
- Heidelberger, C., Chaudhuri, N. K., Danneberg, P., Mooren, D., Griesbach, L., Duschinsky, R., ... Scheiner, J. (1957). Fluorinated pyrimidines, a new class of tumour-inhibitory compounds. *Nature*, 179(4561), 663–666.
- Higuchi, T., & Ikeda, M. (1974). Rapidly dissolving forms of Digoxin: Hydroquinone complex. *Journal of Pharmaceutical Sciences*, 63(5), 809-811.
- Hong, J., -Y., Kim, J. -K., Song, Y., -K., Park, J. -S., & Kim, C. -K. (2006). A new self-emulsifying formulation of itraconazole with improved dissolution and oral absorption. *Journal of Controlled Release*, 110, 332-338.
- Horie, N., Aiba, H., Oguro, K., Hojo, H., & Takeishi, K. (1995). Functional analysis and DNA polymorphism of the tandemly repeated sequences in the 5'-terminal regulatory region of the human gene for thymidylate synthase. *Cell Structure and Function*, 20, 191-197.
- Hou, T., Wang, J., Li, Y., & Wang, W. (2011). Assessing the performance of the mm / pbsa and mm / gbsa methods . 1 . The accuracy of binding free energy calculations based on molecular dynamics simulations. *Journal of Chemical Information and Modelling*, 51, 69–82.
- Houghton, J. A., Maroda, S. J., Phillips, J. O., & Houghton, P. J. (1981). Biochemical determinants of responsiveness to 5-fluorouracil and its derivatives in xenografts of human colorectal adenocarcinomas in mice. *Cancer Research*, 41(1), 144-149.
- Hryniuk, W. M. (1975). The mechanism of action of methotrexate in cultured L5178Y leukemia cells. *Cancer Research*, 35(4), 1085-1092.
- Hubbard, R. E., & Murray, J. B. (2010). Experiences in fragment-based lead discovery. *Methods in Enzymology*, 493, 509-531.

- Huth, J. R., Park, C., Petros, A. M., Kunzer, A. R., Wendt, M. D., Wang, X., ... Chen, J. (2007). Discovery and design of novel HSP90 inhibitors using multiple fragment-based design strategies. *Chemical Biology & Drug Design*, 70(1), 1-12.
- Jackman, A. L., Gibson, W., Brown, M., Kimbell, R., & Boyle, F. T. (1993). The role of the reduced-folate carrier and metabolism to intracellular polyglutamates for the activity of ICI D1694. In Rustum Y.M. (Eds.), *Novel approaches to selective treatments of human solid tumors* (pp. 265-276). Boston, MA: Springer.
- Jackman, A. L., Jodrell, D. I., Gibson, W., & Stephens, T. C. (1991). ICI D1694, An inhibitor of thymidylate synthase for clinical study. In R. A. Harkness, G. B. Elion, & N. Zöllner (Eds.), *Purine and pyrimidine metabolism in man vii: part a: chemotherapy, ATP depletion, and gout* (pp. 19-23). Boston, MA: Springer.
- Javanskar, A., Somwangthanaroj, A., Shao, Z. J., & Rodriguez-Hornedo, N. (2006). Cocrystal formation during cogrinding and storage is mediated by amorphous phase. *Pharmaceutical Research*, 23, 2381-2392.
- Ji, B. T., Devesa, S. S., Chow, W. H., Jin, F., & Gao, Y. T. (1998). Colorectal cancer incidents trends by subsite in Urban Shanghai, 1972-1994. *Cancer Epidemiology, Biomarkers and Prevention*, 7, 661-666.
- Jorgensen, W. L. (1983). Theoretical studies of medium effects on conformational equilibria. *The Journal of Physical Chemistry*, 87(26), 5304-5314.
- Ju, J., Pedersen-Lane, J., Maley, F., & Chu, E. (1999). Regulation of p53 expression by thymidylate synthase. *Proceedings of the National Academy of Sciences of the United States of America*, 96(7), 3769-3774.
- Kim, S. -L., Kim, S. H., Trang, K. T. T., Kim, I. H., Lee, S. -O., Lee, S. T., ... Kim, S. -W. (2013). Synergistic antitumor effect of 5-fluorouracil in combination with parthenolide in human colorectal cancer. *Cancer Letters*, 335(2), 479-486.
- Kollman, P. A., Massova, I., Reyes, C., Kuhn, B., Huo, S., Chong, L., ... Cheatham, T.E. (2000). Calculating structures and free energies of complex molecules: Combining molecular mechanics and continuum models. *Accounts of Chemical Research*, 33, 889-897.
- Kuriki, K., & Tajima, K. (2006). The increasing incidence of colorectal cancer and the preventive strategy in Japan. *Asian Pacific of Journal Cancer Prevention*, 7, 495-501.
- Lamont, E. B., & Schilsky, R. L. (1999). The Oral Fluoropyrimidines in Cancer Chemotherapy. *Clinical Cancer Research*, 5(9), 2289-2296.
- LeszczynskiJerzy (2005). *Computational chemistry : review of current trend*. USA: World Scientific Publishing Company.
- Li, N., DeGennar, M. D., Liebenberg, W., Tiedt, L. R., Zahn, A. S., Pishko, M. V. & de Villiers, M. M. (2006). Increased dissolution and physical stability of

micronized nifedipine particles encapsulated with a biocompatible polymer and surfactants in a wet ball milling process. *Pharmazie*, 61, 595-603.

- Liao, C., Sitzmann, M., Pugliese, A., & Nicklaus, M. C. (2011). Software and resources for computational medicinal chemistry. *Future Medicinal Chemistry*, 3(8), 1057–1085.
- Lipinski, C. A., Lombardo, F., Dominy, B. W., & Feeney, P. J. (1997). Experimental and computational approaches to estimate solubility and permeability in drug discovery and development settings. *Advanced Drug Delivery Reviews*, 23(1-3), 3-25.
- Liu, M., Jiang, M., Zheng, K., Li, Y., Wu, Z., & Yan, C. (2014). Synthesis and structure of a new mononuclear copper ( II ) complex with 2 , 2 ' -bipyridine and picrate: molecular docking , DNA-binding , and in vitro anticancer activity. *Journal of Coordination Chemistry*, 67, 630-648.
- Longo, G. S., Izzo, J., Chang, Y. M., Tong, W. P., Zielinski, Z., Gorlick, R., ... Bertino, J. R. (1998). Pretreatment of colon carcinoma cells with Tomudex enhances 5-fluorouracil cytotoxicity. *Clinical Cancer Research*, 4(2), 469-473.
- Lu, J. B., Sun, X. B., Dai, D. X., Zhu, S. K., Chang, Q. L., Liu, S. Z., & Duan, W. J. (2003). Epidemiology of gastroenterologic cancer in Henan Province, China. *World Journal of Gastroenterology*, 9, 2400-2403.
- MacKerell, A. D. J., Banavali, N., & Foloppe, N. (2000). Development and current status of the CHARMM force field for nucleic acids. *Biopolymers*, 56(4), 257–265.
- Malet-Martino, M., & Martino, R. (2002). Oncologist clinical studies of three oral prodrugs of 5-fluorouracil. *The Oncologist*, 7(4), 288–323.
- McDonald, I. K., & Thornton, J. M. (1994). Satisfying hydrogen bonding potential in proteins. *Journal of Molecular Biology*, 238(5), 777-793.
- McGaughey, G. B., Gagné, M., & Rappé, A. K. (1998).  $\pi$ -Stacking interactions alive and well in proteins. *Journal of Biological Chemistry*, 273(25), 15458-15463.
- Mobley, D. L., & Dill, K. A. (2009). Binding of small- molecule ligands to proteins: “what you see” is not always “what you get”. *Structure*, 17(4), 489-498.
- Momany, F. A., & Rone, R. J. (1992). Validation of the general purpose QUANTA 3.2/CHARMm force field. *Journal of Computational Chemistry*, 13, 888-900.
- Montfort, W. R., Perry, K. M., Fauman, E. B., Finer-Moore, J. S., Maley, G. F., Hardy, L., & Maley, F. (1990). Structure, multiple site binding, and segmental accommodation in thymidylate synthase on binding dUMP and an anti-folate, *Biochemistry*, 29, 6964– 6977.
- Moran, R. G., Mulkins, M., & Heidelberger, C. (1979). Role of thymidylate synthetase activity in development of methotrexate cytotoxicity. *Proceedings of the National Academy of Sciences*, 76(11), 5924-5928.

- Nadzri, N. I., Sabri, N. H., Lee, V. S., & Abdul Halim, S. N. (2016). 5-Fluorouracil co-crystals and their potential anti-cancer activities calculated by molecular docking studies. *Journal of Chemical Crystallography*, 46(3), 144–154.
- NCSM (2016). *National Cancer Society Malaysia*. Retrieved from <http://www.cancer.org.my/quick-facts/types-cancer/>
- NIH (2015). *National Institutes of Health*. Retrieved from <http://www.cancer.gov/types/colorectal>.
- Onufriev, A., Bashford, D., & Case, D. A. (2004). Exploring protein native states and large-scale conformational changes with a modified generalized born model. *Proteins*, 55(2), 383–394.
- Papamichael, D. (1999). The use of thymidylate synthase inhibitors in the treatment of advanced colorectal cancer: current status. *The Oncologist*, 4, 478–487.
- Pepinsky, R. (1955). Crystal engineering: New concept in crystallography. *Physical Review*, 100, 971.
- Perozzo, R., Folkers, G., & Scapozza, L. (2004). Thermodynamics of protein-ligand interactions: history, presence, and future aspects. *Journal of Receptor and Signal Transduction Research*, 24(1–2), 1–52.
- Pfeiffer, P. (1922). *Organische Molekulverbindungen*, Verlag von Ferdinand enke, Stuttgart.
- Phan, J., Koli, S., Minor, W., Dunlap, R. B., Berger, S. H., & Lebioda, L. (2001). Human thymidylate synthase is in the closed conformation when complexed with dUMP and raltitrexed, an antifolate drug. *Biochemistry*, 40(7), 1897–1902.
- PhRMA (2006). *Pharmaceutical Research and Manufacturers of America, Pharmaceutical Industry Profile 2006*, Washington, D.C: Pharma.
- Ramanathan, D. (2009). *Mass Spectrometry in Drug Metabolism and Pharmacokinetics*. Hoboken, NJ: JohnWiley & Sons, Inc.
- Ranjit, T., Amit, D., William, J., Maya, P. L., Lily, R., & Rodriguez-Hornedo, N. (2013). Pharmaceutical cocrystals and poorly soluble drugs. *International Journal of Pharmaceutics*, 453, 101–125.
- Rasenack, N., Hartenhaur, H., & Muller, B.W. (2003). Microcrystals for dissolution rate enhancement of poorly water-soluble drugs. *International of Journal Pharmaceutics*, 254, 137–145.
- Rutman, R. J., Cantarow, A. & Paschkis, K. E. (1954). The catabolism of uracil *in vivo* and *in vitro*. *Journal of Biological Chemistry*, 210, 321–329.
- Salentin, S., Schreiber, S., Haupt, V. J., Adasme, M. F., & Schroeder, M. (2015). PLIP: fully automated protein-ligand interaction profiler. *Nucleic Acids Research*, 43(W1), W443–W447.

- Salo-Ahen, O. M. H., & Wade, R. C. (2011). The active-inactive transition of human thymidylate synthase: Targeted molecular dynamics simulations. *Proteins*, 79(10), 2886–2899.
- Salomon-Ferrer, R., Götz, A. W., Poole, D., Grand, S. L., & Walker, R. C. (2013). Routine microsecond molecular dynamics simulations with AMBER on GPUs. 2. Explicit solvent particle mesh Ewald. *Journal of Chemical Theory and Computation*, 9, 3878–3888.
- Accelrys Software Inc. (2007). Discovery Studio Client 2.5. San Diego.
- Santi, D. V, McHenry, C. S., & Sommer, H. (1974). Mechanism of interaction of thymidylate synthetase with 5-fluorodeoxyuridylate. *Biochemistry*, 13(3), 471–481.
- Scheithauer, W., McKendrick, J., Begbie, S., Borner, M., Burns, W. I., Burris, H. A., ... Marschner, N. (2003). Oral capecitabine as an alternative to iv 5-fluorouracil-based adjuvant therapy for colon cancer: safety results of a randomized, phase III trial. *Annals of Oncology*, 14(12), 1735–1743.
- Schmidt, G. M. J. (1971). Photodimerization in the solid state. *Pure and Applied Chemistry*, 27, 647–678.
- Schrödinger. (2015). *The PyMOL Molecular Graphics System*. New York, USA.
- Schüller, J., Cassidy, J., Dumont, E., Roos, B., Durston, S., Banken, L., ... Reigner, B. (2000). Preferential activation of capecitabine in tumor following oral administration to colorectal cancer patients. *Cancer Chemotherapy and Pharmacology*, 45(4), 291–297.
- Sprous, D. G., Palmer, R. K., Swanson, J. T., & Lawless, M. (2010). QSAR in the pharmaceutical research setting: QSAR models for broad, large problems. *Current Topics in Medicinal Chemistry*, 10(6), 619–637.
- Susnow, R. G., & Dixon, S. L. (2003). Use of robust classification techniques for the prediction of human cytochrome P450 2D6 inhibition. *Journal of Chemical Information and Computer Sciences*, 43(4), 1308–1315.
- Talele, T. T., Khedkar, S. A., & Rigby, A. C. (2010). Successful applications of computer aided drug discovery: Moving drugs from concept to the clinic. *Current Topics in Medicinal Chemistry*, 10(1), 127–141.
- Tamura, K., Ishiguro, S., Munakata, A., Yoshida, Y., Nakaji, S., & Sugawara, K. (1996). Annual changes in colorectal carcinoma incidence in Japan, analysis of survey data on incidence in aomori prefecture. *Cancer*, 78, 1187–1194.
- Torchilin, V. (2007). Micellar nanocarriers: Pharmaceutical perspective. *Pharmaceutical Research*, 24, 1–6.
- Triest, B. V., & Peters, G. C. (1999). Thymidylate synthase: A target for combination therapy and determinant of chemotherapeutic response in colorectal cancer. *Oncology*, 57, 179–194.

- Umeda, Y., Fukami, T., Furuishi, T., Suzuki, T., Tanjoh, K., & Tomono, K. (2009). Characterization of multicomponent crystal formed between indomethacin and lidocaine. *Drug Development and Industrial Pharmacy*, 35, 843-851.
- Van Cutsem, E., Cunningham, D., Maroun, J., Cervantes, A., & Glimelius, B. (2002). Raltitrexed: Current clinical status and future directions. *Annals of Oncology*, 13(4), 513-522.
- Van Cutsem, E., Köhne, C. H., Láng, I., Folprecht, G., Nowacki, M. P., Cascinu, S., ... Schlichting, M. (2011). Cetuximab plus irinotecan, fluorouracil, and leucovorin as first-line treatment for metastatic colorectal cancer: updated analysis of overall survival according to tumor KRAS and BRAF mutation status. *Journal of Clinical Oncology*, 29(15), 2011-2019.
- van Gunsteren, W. F., & Berendsen, H. J. C. (1977). Algorithms for macromolecular dynamics and constraint dynamics. *Molecular Physics*, 34(5), 1311-1327.
- Van Triest, B., & Peters, G. J. (1999). Thymidylate synthase: A target for combination therapy and determinant of chemotherapeutic response in colorectal cancer. *Oncology*, 57(3), 179-194.
- Van Triest, B., Pinedo, H. M., Van Hensbergen, Y., Smid, K., Telleman, F., Schoenmakers, P. S., ... Peters, G. J. (1999). Thymidylate synthase level as the main predictive parameter for sensitivity to 5-fluorouracil, but not for folate-based thymidylate synthase inhibitors, in 13 nonselected colon cancer cell lines. *Clinical Cancer Research*, 5(3): 643-654.
- Vanquelef, E., Simon, S., Marquant, G., Garcia, E., Klimerak, G., Delepine, J. C., Cieplak, P. and Dupradeau, F. (2011). R.E.D. server: A web server for deriving RESP and ESP charges and building force field libraries for new molecules and molecule fragment. *Nucleic Acids Research*, 39, W511-517.
- Venkataramana, C. H. S., Ramya Sravani, K. M., Swetha Singh, S., & Madhavan, V. (2011). In-silico ADME and toxicity studies of some novel indole derivatives. *Journal of Applied Pharmaceutical Science*, 1(10), 159-162.
- Walsh, R. D. B., Bradner, M. W., Fleishchman, S., Morales, L. A., Moulton, B., Rodriguez-Hornedo, N. & Zaworotko, M. J. (2003). Crystal engineering of the composition of pharmaceutical phases. *Chemical Communication*, 6, 186-187.
- Wang, J., Wang, W., Kollman, P. A., & Case, D. A. (2004). Development and testing of a general amber force field. *Journal of Computational Chemistry*, 25, 1157-1174.
- Ward, W. H. J., Kimbell, R., & Jackman, A. L. (1992). Kinetic characteristics of ICI D1694: A quinazoline antifolate which inhibits thymidylate synthase. *Biochemical Pharmacology*, 43(9), 2029-2031.
- WHO (2011). *World Health Organization*. Retrieved from [http://www.who.int/medicines/areas/quality\\_safety/quality\\_assurance/Definition\\_API-QAS11-426Rev1-08082011.pdf](http://www.who.int/medicines/areas/quality_safety/quality_assurance/Definition_API-QAS11-426Rev1-08082011.pdf)

- Wilkinson, A. J., Fersht, A. R., Blow, D. M., Carter, P., & Winter, G. (1984). A large increase in enzyme-substrate affinity by protein engineering. *Nature*, 307(5947), 187–188.
- Wilson, P. M., Danenberg, P. V, Johnston, P. G., Lenz, H.-J., & Ladner, R. D. (2014). Standing the test of time: Targeting thymidylate biosynthesis in cancer therapy. *Nature Publishing Group*, 11(5), 282–298.
- Wohler, F. (1844). Untersuchungen Uber Das Chinon. *Annalen*, 51, 153.
- Yadav, A. V., Shete, A. S., Dabke, A. P., Kulkarni, P. V., & Sakhare, S. S. (2009). Co-crystals: A novel approach to modify physicochemical properties of active pharmaceutical ingredients. *Indian Journal of Pharmaceutical Science*, 71(4): 359–370.
- Yang, L., Parkin, D. M., Li, L. D., Chen, Y. D. & Bray, F. (2004). Estimation and projection of the national profile of cancer mortality in China: 1991-2005. *British Journal of Cancer*, 90, 2157-2166.
- Yee, Y. K., Tan, V. P., Chan, P., Hung, I. F., Pang, R. & Wong, B. C. (2009). Epidemiology of colorectal cancer in Asia. *Journal of Gastroenterology and Hepatology*, 24, 1810-1816.
- Yiu, H. Y., Whittemore, A. S. & Shibata, A. (2004). Increasing colorectal cancer incidence rates in Japan. *International Journal of Cancer*, 109, 777-781.
- Yue, X., Qiao, Y., Qiao, N., Guo, S., Xing, J., Deng, L., Xu, J. & Dong, A. (2010). Amphiphilic methoxy polyethylene glycol-b-poly( $\epsilon$ -caprolactone)-b-poly –(2-dimethylaminoethyl methacrylate) cationic copolymer nanoparticles as a vector for gene and drug delivery. *Biomacromolecules*, 11, 2306-2312.
- Yun, J. -A., Kim, H. C., Son, H.-S., Kim, H. R., Yun, H. R., Cho, Y. B., ... Chun, H.-K. (2010). Oncologic outcome after cessation or dose reduction of capecitabine in patients with colon cancer. *Journal of the Korean Society of Coloproctology*, 26(4), 287–292.

## LIST OF PUBLICATIONS AND PAPERS PRESENTED

- Sabri, N. H., Abdul Halim, S. N., Sharifuddin, M. Z., & Lee, V. S., (2018). Modification of anti-cancer co-crystal for thymidylate synthase inhibition: Molecular dynamics study. *Chiang Mai Journal of Science*, 45(x), 1-13.
- Nadzri, N. I., Sabri, N. H., Lee, V. S., & Abdul Halim, S. N. (2016). 5-Fluorouracil co-crystals and their potential anti-cancer activities calculated by molecular docking studies. *Journal of Chemical Crystallography*, 46(3), 144–154.

University of Malaya